UiT
THE ARCTIC
UNIVERSITY
OF NORWAY

Faculty of Biosciences, Fisheries and Economics

A Patch of *Calanus finmarchicus* in the Lofoten-Vesterålen Region

Characteristics and determining factors

—

Néstor Santana Hernández

BIO-3950 Master thesis in Biology … May 2019

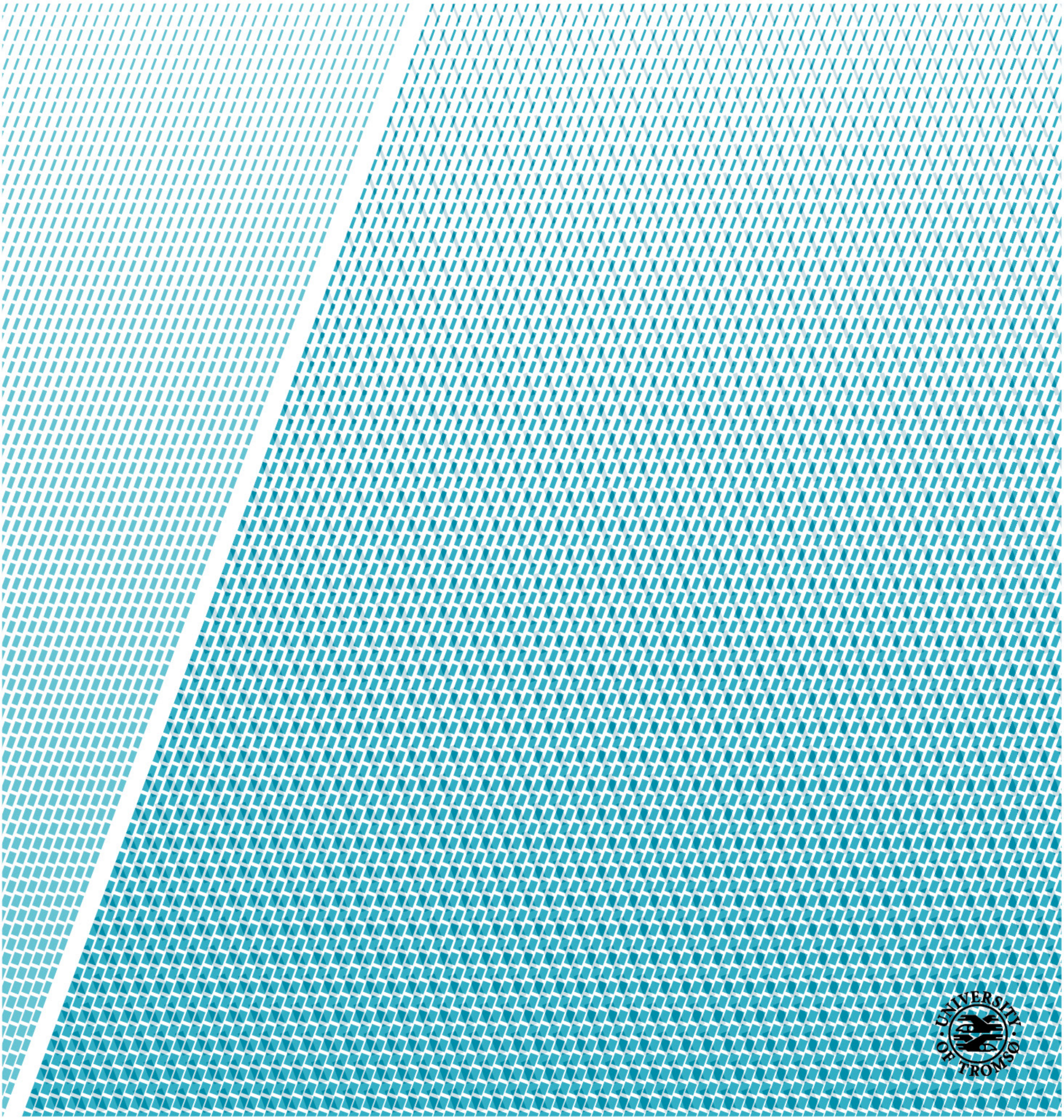

Abstract

Zooplankton patchiness has been documented in many shelf areas and is of vital importance for understanding predator-prey relationships in pelagic marine systems. By combining hydrographic, acoustic and net data collected in spring 2017, we present a detailed understanding of the extent of this phenomenon in the Lofoten-Vesterålen region. Such patches are of potential interest not only for zooplankton harvesting, but also for commercially harvested species such as Atlantic Cod, which are crucial for the region's economy. We hereby report evidences of a large surface patch (>1000 km^2) of *Calanus finmarchicus* extending longitudinally over the whole continental shelf. The aggregation was closely tied to the water mass distribution in the area together with the timing of the bloom and its associated ascent of the overwintering copepod population. Although most organisms concentrated at surface, species-specific depth preferences resulted in statistically definite communities at diverse depths. Despite the low chlorophyll *a* values, high nutrient concentrations proved optimum conditions for phytoplankton development and significantly matched with the zooplankton distribution. We thus hypothesize that top-down control via intensive grazing pressure plays a significant role in regulating both the bloom's size and the related surface aggregation of zooplankton. This paper will assess the dimentions, morphology and composition together with possible physical and biological drivers of zooplankton patches to provide a highly comprehensive view of the distribution of this copepod, its aggregating behaviour and its ecological importance.

Keywords: *Calanus finmarchicus,* zooplankton patchiness, Lofoten-Vesterålen, bioacoustics, spring bloom, Norwegian Coastal Current

Abbreviations

AIW	Arctic Intermediate Water
ANOVA	Analysis of Variance
AW	Atlantic Water
BEST	Bioenv and Stepwise
CTD	Conductivity, Temperature, Density
DSD	Depth Standard Deviation
GPS	Global Positioning System
LSD	Least Significant Distance
LOPC	Laser Optical Plankton Counter
MAD	Mean Acoustic Density
MASD	Mean Acoustic Species Density
MDS	Multidimensional Scaling
MPD	Mean Patch Depth
NAC	Norwegian Atlantic Current
NCC	Nowegian Coastal Current
PL	Prosome Length
PP	Primary Production
R	Roughness
SA	Surface Area
SSL	Sound Scattering Layer
Sv	Backscattering Coefficient
SW	Shannon Wiener
TS	Target Strength
V	Volume
VPR	Video Plankton Recorder

Table of Contents

1 Introduction

1.1 Zooplankton Patchiness

The way organisms occupy space is the result of physical and biological drivers influencing the environment and the interactions between individuals. However, regional differences in physiology, life history and ecological characteristics also have an important repercussion in distribution patterns. Although poorly characterized and understood (Franks, 2005), the distribution of both phytoplankton and zooplankton has been observed to be patchy in many shelf areas (Gallager et al., 1996). Patchiness is defined as a discontinuous distribution of individual organisms through space and is often a result of the interaction between physical and biological processes (Haury et al., 1978). Phytoplankton, bacteria, marine snow and zooplankton form thin plankton layers (Benoit-Bird et al., 2010). Concentrations of plankton and particles within patches are by definition higher than in the background waters. Thus, they are normally defined by a concentration of individuals exceeding the median value. Such aggregations can arise as responses to temperature and salinity gradients or discontinuities, water motion, variation in light intensity, food and/or predator concentrations as well as from complex social and reproductive behaviours (Ambler, 2002). Since these structures can affect catchability by predators and fishers, understanding this phenomenon is of high relevance for ecological and economical reasons.

The biological importance of zooplankton patchiness resides in the relevance of these key trophic players in the transfer of primary production (PP) to top predators such as fish, marine mammals and seabirds, meaning such aggregations have the ability to enhance trophic transfer (Wishner et al., 1988). The fine-scale spatial distribution of prey is of high relevance to how predators evaluate the suitability of their food supply and the mechanisms they use to exploit it (Benoit-Bird et al., 2013). This means the survival and growth of many zooplankton predators, from invertebrates to whales, depends on their success in finding rich patches of prey, as the ambient abundances of zooplankton outside these patches are often too low to maintain previously observed rates of predator growth and reproduction (Genin et al., 2005). Hence, prey patch characteristics such as location in the water column and local density within spatial aggregations heavily influence habitat use by predators, suggesting patchiness may be of vital importance for understanding predator-prey relationships in pelagic marine systems (Benoit-Bird et al., 2013).

The ecological consequences of any patch formation will depend on the intensity, size and persistence of the aggregations. Patches can differ greatly in terms of their size, shape and generating processes, their species and size-specific compositions, as well as the concentrations of individuals within aggregations. The size of plankton patches and their variability generally scale inversely with the organism's size (Levin, 1992). Large patches are known to spread horizontally over many kilometres, that is between 30 and 60 km or even >100 km in case of the largest patches (Pinca and Huntley, 2000). Persistence of such patches in off-shore waters can be frequently measured in weeks or months (Cushing and Tungate, 1963).

1.2 Patch Formation

The relative importance of physical vs. biological processes to zooplankton patch formation cannot be determined a priori and may shift in magnitude with time (Stacey et al., 2007). Aggregation implies an increase in concentration, which can often have a biological factor at its source. Nevertheless, in marine ecosystems, pelagic fish and plankton spatial distributions in ocean ecosystems are highly influenced by hydrologic features such as ocean fronts, eddies, thermal stratification and upwelling (Mann and Lazier, 1996). As a result of the interaction between animal behaviour and these physical processes, large patches of zooplankton develop and are maintained. The habitats seem to be confined within hydrographic structures that aggregate the animals in restricted areas, resulting in 'hotspots' with high abundances of zooplankton that are found in the same areas from year to year (Halvorsen et al., 2003).

Although biological processes such as feeding, reproduction and predator avoidance strategies may be of greater interest, Gaardsted et al. (2010) proved the importance of also quantifying variability due to advection. They reported an estimated transport of copepods through the study area boundaries corresponding to a rate of change of 7% day^{-1} off the shelf of northern Norway, which clearly illustrates the relevant consequences of coupling between mesoscale currents and patchiness in the zooplankton distribution. Surface waters involve strong surface circulation that may disperse its inhabitants over large distances (Halvorsen et al., 2003), suggesting organisms could possibly aggregate to enhance their chances of survival. This means an accurate description of plankton distributions and dynamics is often not achievable without considering advection effects. Thus, evaluating heterogeneity in zooplankton abundance and its relationship with currents is critical, although special attention must be paid to separate population variability at a given location due to advection from other zooplankton dynamics (Gaardsted et al., 2010).

1.3 The North Atlantic Key Species, *Calanus finmarchicus*

With an annual biomass production of 150-300 million tons in the Nordic Seas, frequently constituting > 50% of mesozooplankton biomass throughout the North Atlantic (Melle et al., 2014), the planktonic copepod *Calanus finmarchicus* is the dominating grazer in the Lofoten-Vesterålen region (Planque and Batten, 2000). It is one of the most important multicellular zooplankton species in the northern North Atlantic, based on its abundance and role in food webs and biogeochemical cycles. The distribution of this calanoid copepod, described by Wishner et al. (1988) as very patchy, is sizeably influenced by circulation systems and their associated water mass characteristics. From the basin-wide programs, in combination with local time series measurements and Continuous Plankton Recorder (CPR) surveys, a tremendous source of information and knowledge of *C. finmarchicus* distribution and life history traits has emerged. This makes it a well-studied species, subject of a book (Marshall and Orr, revised edition, 1972) and over 1000 research articles since its publication (Melle et al., 2014). However, few studies have addressed patchiness of this species, and considering its dominance of the zooplankton assemblage in the study area, we can assume it is highly relevant in the composition of zooplankton patches on a large scale.

This copepod plays an important role in the structure, stability, and function of marine ecosystems on the Norwegian continental shelf (Sakshaug et al., 1994). Numerous planktivorous fish species, such as the Atlantic mackerel *(Scomber scombrus)*, Atlantic herring *(Clupea harengus)* and Capelin *(Mallotus villosus)* feed on plankton fields with *C. finmarchicus*. These are commercial fish species commonly harvested by the Norwegian fishery industry, meaning *C. finmarchicus* and its key position in the trophic chain are of high economic and commercial relevance, such that the famous Norwegian marine biologist A. Boeck wrote “It is hard to imagine that such minute animals could be of such importance in the economy of a country”.

During its annual life cycle from egg to adult, *C. finmarchicus* pass through six nauplius (NI–NVI) and five copepodite stages (CI–CV) *(Figure 1)*. Individuals enter dormancy in summer and fall (Hirche, 1996a), constituting a major part of the spawning population the following spring. They carry with them lipid stores that make up most of their body weight and sustain metabolism during overwintering and subsequent molting, and partial development of gonads in mid-late winter (Rey-Rassat et al., 2002). Dormant copepodites are characterised by reduced metabolism and slowed development (Saumweber and Durbin, 2006). Enhanced probabilities of survival because of lower temperatures, and the avoidance of predators and parasites are considered the main advantages of overwintering at depth (Krause and Radach, 1989). However, this deep water hibernation strategy also allows *C. finmarchicus* to reduce its loss rates due to advective dispersal during winter. As shown in figure 3, the main overwintering stage is the pre-adult CV (Conover, 1988), most abundant between 600 and 1200 m, well below the reach of surface-orientated planktivores, and at temperatures below 2°C in the Norwegian Sea (Edvardsen et al., 2006). Ascent from the winter diapause generally occurs in mid-late winter, when most CVs leave dormancy, molt into adults and mate upon returning to the surface (Melle et al., 2004). Overwintering populations of diverse origin concentrate over the continental shelf outside the Lofoten Islands to feed and spawn during the phytoplankton spring bloom, forming surface layers with high abundances. Such layers could represent an important food item probably governing the migration of the herring (Melle et al., 1994; Huse et al., 2012)

The spring distribution of *C. finmarchicus* nauplii reflects spawning events occurring immediately after the seasonal ascent migration from deep hibernation habitats, where copepodite stage CV dwells for overwintering (Broms et al., 2016). Females then lay eggs in response to food levels, for which chlorophyll *a* concentration is a useful proxy (Runge et al., 2006). During the surface-dwelling period of the life cycle, mortality appears to be greatest. Highest rates affect the earliest stages (eggs, nauplii) (Aksnes and Magnesen, 1988), where it is especially important in determining overall recruitment success (Ohman and Hirche, 2001; Ohman et al., 2002). Following the nauplii stage, the maximum abundance of CIs of the first generation is often observed to occur during the peak of the bloom or slightly after (Melle et al., 2004). For the first three copepodite stages (CI – CIII) individuals will remain in the upper mixed layer or within the pycnocline, if a subsurface chlorophyll maximum develops during the post-bloom phase (Melle et al., 2004). Survivorship of these stages is a key factor in the *C. finmarchicus* population dynamics, as it will determine the number of further new generation CV individuals migrating to overwintering areas after the bloom. It is conditioned by environmental factors such as temperature, food availability and con-specific abundance, resulting in marked seasonal and regional variability in stage-specific mortality patterns (Ohman and Hirche, 2001; Ohman et al., 2002).

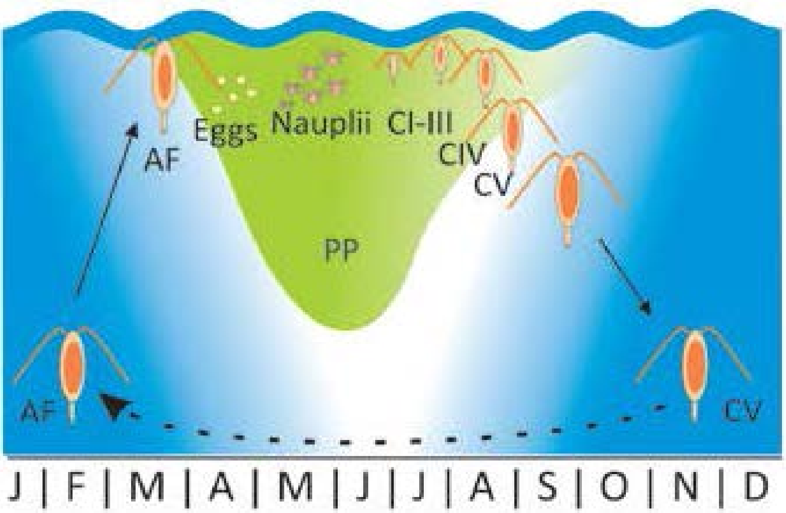

Figure 1: Conceptual life cycle of Calanus (CI-CV: copepodite stages I-V; AF: adult female) (Figure: Malin Daase)

1.4 Research area

Located between 67°21’ and 69°23’ North and 11°44’ and 16°16’ East *(Figure 2)*, the Lofoten-Vesterålen marine ecosystem is extremely rich in biodiversity and is a key area for fish species of high commercial and ecological relevance, such as Atlantic cod *(Gadus morhua)* and herring *(Clupea harengus)*. The Lofoten-Vesterålen shelves, contain the main spawning grounds for the Arcto-Norwegian cod stock (Ottersen et al., 2014). Such fishery resources are an important part of local tradition and culture since the Viking ages and the fishing industry in the area is of high economic importance to the local population. Patches of *C. finmarchicus* have been observed in the area regularly, playing a key role as source of food for commercial fish species due to their position in the trophic chain. Moreover, many seabirds breed in the area and high numbers of marine mammals are observed, making it an area of high ecological importance. These top predators are dependent on *C. finmarchicus*, which funnels PP to higher trophic levels. A recent and promising fishery aimed at developing a variety of products for human consumption is also based on this copepod. Thus, increasing knowledge concerning the productivity of this key trophic player will help to protect fish stocks and thus guarantee the continuity of the fishing industry in the area. One of the main challenges for the area is to ensure that existing fishery activities together with increasing maritime transport and the tourism industry do not negatively impact such a valuable ecosystem. Therefore, the region has been designated as one of the seven ‘especially valuable and vulnerable areas’ by the Norwegian government (“Integrated Management Plan for the Marine Environment”, 2011).

1.4.1 Climate and Oceanography

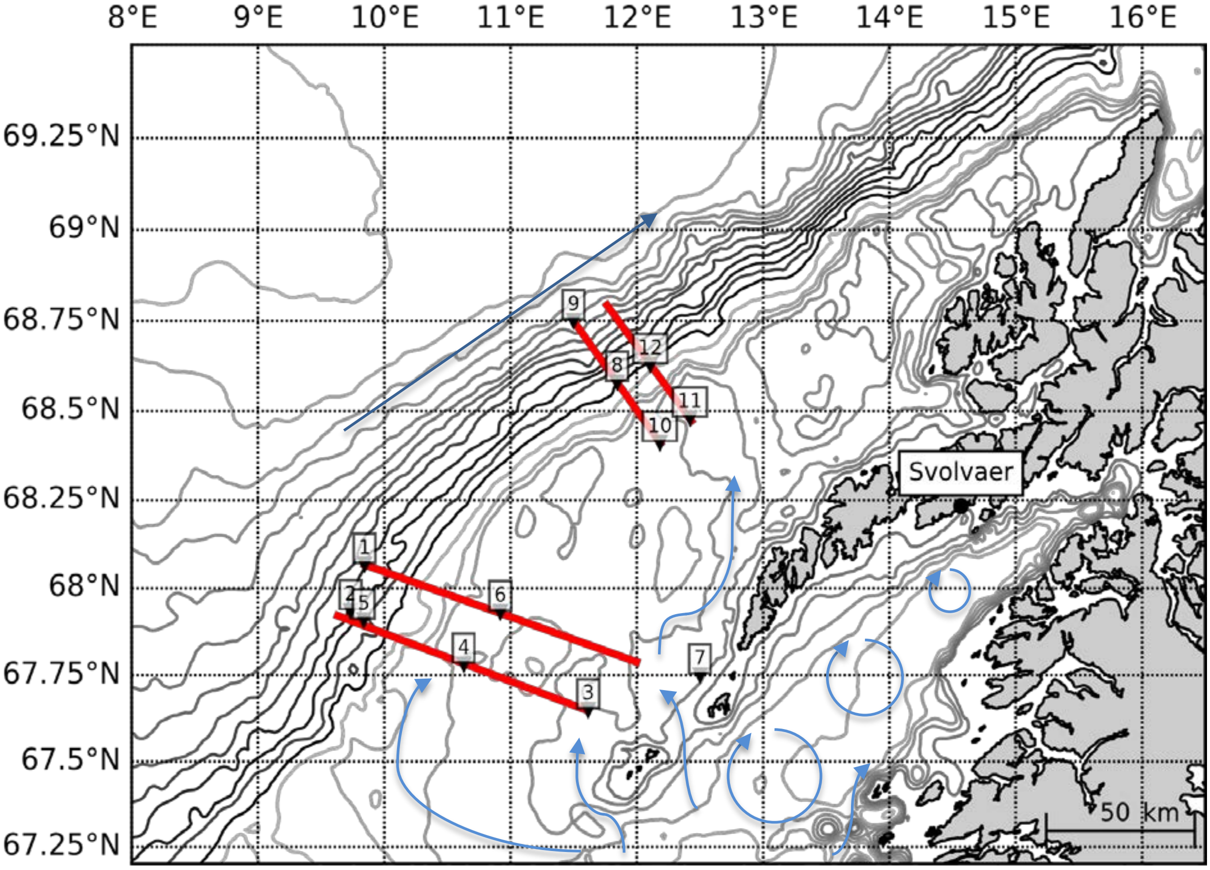

Figure 2: Map of theresearch area. Red lines mark the acoustic transects conducted across the patch from South to North: S2, S1, S3 and S4. The numbers show the location of the different stations, including test stations 1 to 3. The light blue arrows represent the Norwegian Coastal Current (NCC) and the dark blue arrow represents the Norwegian Atlantic Current (NAC).

The Lofoten-Vesterålen area presents complex hydrographic features *(Figure 2)*. The current system, together with the bathymetry, atmospheric conditions, and freshwater discharge, create considerable differences in the physical and biological environment of the continental shelf, the shelf-break, and the open ocean (Pedersen et al., 2000).

The complex bathymetry of the region, characterised by deep troughs separating well-defined banks, to a great extent determines the circulation pattern, residence time and water mass exchange (Sundby, 1984), meaning there is a strong topographic influence in the flow regime of the study area. As we move offshore, it varies from Vestfjorden, an atypical fjord with a very wide opening and no well-defined sill, to a relatively shallow continental shelf (ca. 150 m.) and a steep shelf break descending to the deep Lofoten basin *(Figure 2)*. Off Lofoten-Vesterålen the continental shelf is narrow (ca. 65 km) such that the frontal system is found close to the coast. In addition, the narrow sounds and straits between the main Lofoten Islands, where strong currents such as the famous Moskenesstraumen can be found, connect Vestfjorden with the shelf areas off the western coast of the archipelago, developing an important fjord-shelf water exchange driven by strong tidal currents.

Circulation in the area is dominated by two major northward flowing currents, the Norwegian Atlantic Current (NAC) and the Norwegian Coastal Current (NCC) (Sætre, 1999) *(Figure 2)*. Strongly steered by topography, the saltier NAC runs northward to the west of the NCC and further offshore, along the shelf-break (Gascard et al., 2004). It is responsible for the inflow of warm and saline Atlantic Water (AW) into the Arctic, occupying the upper 600–700 m of the water column. A salinity minimum associated with a layer of Arctic Intermediate Water (AIW) is found below the AW (Blindheim, 1990), separating the AW from the deep water. The NCC flows along the coast, over the continental shelf. It divides into two branches south of Vestfjorden, one continuing north into the fjord to join the circulation system inside and the other steering west around the Lofoten tip before continuing northwards along the northwest coast of the Lofoten Islands *(Figure 2)*. The front between both currents is usually sharp and located near the shelf break, resulting in a restricted cross-shelf water exchange throughout the year, especially during winter, when the NCC is strongest (Gaard and Hansen, 2000). Furthermore, the dynamic nature of the northward flowing NCC and the strong topographic influence of the flow regime in the area are likely to be the main driving forces in the formation of deep-water mesoscale anticyclonic eddies, which are frequently formed along the continental slope and in the Lofoten Basin.

The oceanography of the area is subject to high seasonal and spatial variability. Changing hydroclimatic conditions over the seasons result in different circulation patterns over the shelf. For example, during winter, the NCC has a narrower and deeper (ca. 50– 150 m) wedge-shape and flows faster than in summer due to the prevailing southerly winds. Such winds can pile up water masses towards the coast due to the effect of inshore Ekman transport, enhancing the barotropic component of the current and thus increasing its strength (Mitchelson-Jacob and Sundby, 2001). In these periods where the current is stronger, it flows closer to the coast. This results in the advection of colder water masses near the entrance of fjords located upstream of Vestfjorden, before the NCC splits, directly to the shelf areas situated off the north-western coast of the Lofoten Islands. Spatial variability within the study area includes differences in the physical conditions of the water masses, most evident along an east–west axis. Cold, low-salinity water near the coast contrasts with AW masses dominating at the continental slope and in the open ocean (Pedersen et al., 2000). In summer, the seasonal lateral movement mixes both water masses, eroding the clearly defined gradients present in spring. This complex circulation system will strongly affect the plankton distribution around the Lofoten Islands by continuous advection of planktonic organisms (Espinasse et al, 2016).

1.4.2 Production Regimes

The North Atlantic pattern of PP is mainly determined by light conditions and surface temperatures, but also nutrient supply, mechanisms of water column vertical stabilisation and grazing. The northeast Atlantic represents a typical spring bloom system, although variations between deep basins and shelf areas exist within the seasonal cycle of PP. According to Sverdrup's critical depth concept, production occurs when the mixing depth of algal cells is less than a critical depth such that net production is positive (Sverdrup, 1953). This usually occurs in March–April, allowing the bloom to start shortly after, when the pycnocline approaches the upper 30– 40 m (Zhai et al., 2012). Sverdrup's concept of critical depth has been shown to accurately address the pattern of seasonal phytoplankton production in the Norwegian Sea, although recent publications point to more complex or at least regionally different controlling mechanisms (Behrenfeld, 2010; Mahavedan et al., 2012).

Large seasonal and spatial variability of chlorophyll *a* has been observed by Pedersen et al. (2000) in the study area, and interannual variations in the timing of the bloom are common (Rey, 2004). However, by early April, PP has normally started with chlorophyll *a* values in the range between 2–4 mg/L in the surface layer (0–20 m) and by May/June the accumulation of chlorophyll *a* has increased around 0.8 mg/L, mainly at surface waters along the shelf-edge (Pedersen et al., 2000). These chlorophyll concentrations in the upper mixed layer are however lower than 3 mg/L in average (Bagoeien et al., 2012). Nonetheless, maximum chlorophyll concentrations regularly correspond to maximum phytoplankton production, both occurring near the surface. This scenario attracts grazer species such as *C. finmarchicus*, meaning maximum abundances of this copepod could also be related to maximum chlorophyll concentrations and phytoplankton production (Longhurst and Harrison, 1989).

1.5 Rationale and Objectives

Several studies (e.g., Brentnall et al., 2003) have suggested that patches of plankton are essential to the growth and survival of planktonic species such as Atlantic cod *(Gadus morhua)*, Hence, understanding the extent of this phenomenon in the distribution of species could be of potential interest not only for zooplankton harvesting but also its main predators, as it plays a key role in the trophic web to commercially exploited fish species. Thus, due to their important role in the ecosystem, sustainable management based on scientific studies concerning their productivity is critical to protect their stocks.

Unfortunately, sampling difficulties have left knowledge of their structure and mechanisms of their formation in free-living populations incomplete, remaining a central issue in marine ecology. Zooplankton patches have been previously approached using a wide range of methods such as net sampling, continuous water pumping, acoustics, optical counters, video recording, automated underwater vehicles, laboratory experiments or modelling (Geoffroy et al., 2016; Trudnowska et al., 2016). Despite the high research efforts, difficulties to obtain appropriate spatial resolution and distinct differentiation between a patch and the ambient water have resulted in a poor understanding of this phenomenon. Similarly, the large spatial scale in oceanic systems and the lack of consistent methods for acoustically distinguishing fish shoals from plankton patches have allowed only a limited study of the spatial interrelationship of fish and zooplankton in the open ocean (Swartzman et al., 1999).

Most of these studies have focused on the vertical distribution of organisms in the water column rather than on their horizontal distribution. One of the main goals when addressing this topic is linking aggregative processes and their influence across spatial scales (Folt and Burns, 1999). This enhances the need for an interdisciplinary study able to locate patches and delineate physical and behavioural mechanisms responsible for zooplankton patch formation in the ocean. These knowledge gaps have motivated a study involving a scientific cruise conducted in spring 2017 in the Lofoten-Vesterålen region with the aim of determining the physical and biological mechanisms responsible for the formation of zooplankton patches, and how these influence stock size estimations of a commercially harvested key species. By describing patches of *C. finmarchicus* in detail based on acoustic and net sample data, and further relating patch structure to environmental drivers, this thesis contributes to a better understanding of the species dynamics and behaviour, but also that of its main predators.

2 Materials and Methods

2.1 Hydrographic Sampling

A SBE 911+ CTD equipped with sensors for conductivity (salinity), temperature, pressure (depth), oxygen, fluorescence and turbidity together with 12 x 5 L Niskin bottles for water sampling was deployed 12 times along the transects *(Figure 2)*. CTD profiles were taken along the whole water column down to depths ranging from 97 m at the shallowest station to 2183 m at the deepest station. In addition, to obtain a high spatial resolution of data on water mass properties, an Applied Microsystems Micro CTD was mounted on the Moving Vessel Profiler and recorded Temperature-Salinity profiles along the acoustic transects. This allowed us to measure the spatial and vertical variability in temperature and salinity in the water column and later interpret the effects of these key physical factors on zooplankton patchiness. In addition, the CTD data enabled the calculation of the equivalent sound speed and coefficients of absorption required for the acoustic data analysis.

Nutrient (Bottom, 50, 20, 10, 5 and 0 m) and chlorophyll *a* (50, 20, 10, 5 and 0 m) samples were taken at all stations except station 3. Chlorophyll *a* samples were filtered on board using GF/F filters (3 parallels per station with 50 to 150 ml filtered per parallel) and conserved at -80°C together with the nutrient samples for further analysis on land. An overview of all CTD stations and water samples is given in the appendix.

2.2 Acoustic Sampling

The EK60 multifrequency echosounder was keel-mounted on *R/V Helmer Hanssen*, calibrated prior to departure with the standard sphere method (Simmonds and MacLennan, 2005) and continuously recorded acoustic data at 38 and 120 kHz along the entire cruise track. The results described in this report will focus on the transects conducted across the observed patch. In order to target the complete zooplankton community in the water column, ideally a higher frequency such as 200 kHz should have been used. Unfortunately this transducer was not available for our cruise, meaning smaller meso and micro-zooplankton species could have eluded detection by the echosounders.

The resulting acoustic data profiles were later scrutinized with the Echoview 7.1 software. The data was cleaned, meaning that bad data, noise and attenuated signals were removed from the analysis. This process requires a high level of precision, as zooplankton can be mistakenly removed as noise. Due to the ship's draft and near field region (Simmonds and MacLennan, 2005), acoustic data from the top 12 m were excluded from the analysis. We understand this is a limitation to our study, since copepods are known to form large patches at the surface (Basedow et al., 2019).

Once the data was ready for analysis, we characterized patches with three metrics:

1) **Mean acoustic density (MAD) and mean acoustic species density (MASD)**

To calculate the volume backscattering strength (Sv in dB re 1 m^{-1}) for every section of the water column, the echograms were gridded into 0.25 nmi of distance by 1 m of depth cells. The backscatter values in each grid box were integrated by cells for the area located between the top line and the line of mean patch depth with the aim of only targeting the organisms located in the patch. Echointegration was also performed for the area located between the line of mean patch depth and the bottom line in order to establish a comparison of the backscatter within and outside the patch. Average Target strength (TS) for each zooplankton species captured in the nets was obtained using the following formulas from the literature:

For gastropods and appendicularians (Stanton et al., 1994):

$$TS = 10log\ \{(\frac{25}{144})\ \pi^4 D^6 f^4 R^2 c^{-4}(1 + (\frac{25}{9})\ \pi^4 f^4 D^4 c^{-4})^{-1}\}$$

Where R = reflection coefficient, 0.05, D = mean body width (m), f = frequency, c = speed of sound.

For fluid-like animals (Copepoda, Amphipoda, Euphausiacea, Decapoda, Chaetognatha) (Stanton et al., 1994):

$$TS = 10^{0.08R^2L^2\beta_D{}^{-1}[1-exp(-8\pi^2f^2D^2s^2c^{-2})cos(\pi fDc^{-1}(4-0.5\pi(\pi fDc^{-1}+0.4)^{-1}))]}$$

Where R = reflection coefficient, 0.038 (Copepoda, Euphausiacea, Decapoda,), 0.056 (Amphipoda), 0.03 (Chaetognatha), L = mean body prosome length (m), s = standard deviation (SD) of length, β_D = ratio of body length to width, D = mean body width (m), f = frequency, c = speed of sound.

For Atlantic cod *(Gadus morhua)* larvae (Chu et al., 2003):

$$TS = 176.1 \log_{10} L - 82.4$$

Where L = mean length (cm)

The average TS for all species combined and average Sv for each transect were then combined to calculate the MAD (all species combined) and MASD (each species) for all transects outside and within the patch.

$$MAD = (10^{Mean\ Sv/10})/Mean\ (10^{Mean\ TS/10})$$

$$MASD = MAD \times Relative\ Abundance\ of\ Each\ Species$$

2) Depth and distance to the vessel

Sv contours at – 73 dB re m^{-1} were used to delimitate the border of a patch. Mean patch depth of the signal within these contours (MD) and depth standard deviation (DSD) were measured.

3) Surface area (SA) and volume (V) of the patch

Length and width were obtained using the GPS positions of the patch's borders throughout the different transects. SA was calculated by joining the borders of the patches at the different transects before calculating the distance in Km between them. To enable easier SA calculation, SA was obtained for triangular sections which were later added together. The following formula was applied, where a, b, c are the distances between the coordinate points that form each triangle:

$$SA\ (Km^2) = A_{t1} + A_{t2} + A_{tn\dots}$$

$$A_{tn} = \sqrt{p_{tn}(p_{tn} - a_{tn})(p_{tn} - b_{tn})(p_{tn} - c_{tn})}$$

$$p_{tn} = (a_{tn} + b_{tn} + c_{tn})/2$$

Patch Volume (V) was calculated multiplying the SA by the previously calculated patch MD using the following formula:

$$V(m^3)\ =\ SA\ x\ MD$$

2.3 Net Sampling

2.3.1 Mulitinet Sampling

A Hydrobios Multinet (0.25 m^2) with a mesh size of 180 µm was deployed at 9 stations located along the acoustic transects to estimate zooplankton abundance and ground truth the acoustic signal. In addition, two electronic flowmeters with automatic angle compensation were mounted on the underwater unit to obtain the volume of water filtered by the net, necessary for the calculation of the abundance (ind/m^3). Samples were taken from 5 depth strata and fixed in 4% formalin-seawater solution (Zoofix) for further analysis on land. An overview of all multinet stations taken is given in the appendix.

Further laboratory analysis consisted of sorting the different samples by species and their developmental stages when possible. At least 450 zooplankton individuals and 100 *Calanus* were identified from each sample. Abundance (ind/m^3) was calculated using the volume of water filtered by the net from the two electronic flowmeters mounted on the multinet. Most length, length SD, width and weight measurements were obtained from a similar study by this author where they were determined experimentally by randomly selecting 30 organisms of each species. Measurements for species with no record were obtained from the literature *(Appendix 2).*

2.3.2 Bongo Net Trawling

A bongo net with a mesh size of 200 and 500 µm was deployed twice at each station except for station 12 to sample Atlantic cod *(Gadus morhua)* larvae, a well-kown predator of copepoda nauplii. The net was towed for 20 minutes at depths ranging from 0 to 30 meters at speeds of 2-3 knots. Stations 10 and 11 were sampled only with the 500 µm net, since the 200 µm net tore due to the harsh weather conditions during station 9, meaning no data was collected for this station. Cod larvae were roughly sorted before preservation in small glass vials with ~80% ethanol solution for later quantification in the laboratory. An overview of all bongo net trawls is given in the appendix.

2.4 Statistical Analysis

The results that one can obtain by statistical analysis are objective and meaningful conclusions that are to be trusted more than descriptive observations. Thus, our data was submitted to a series of statistic tests. An ANOVA test from the general linear models was used to evaluate the significance of the multinet data. Levene's test was used to ensure homogeneity between the variances. If the resulting p value was below 0.05, the variables were converted into logarithmic form. To complete the ANOVA test, the variables were submitted to a Fisher Least Significant Distance (LSD) test, allowing us to assess the significance of the variations within the categorical factors.

Multivariate structure of the zooplanktonic assemblage and its relationship with the physical-biological composition of the water column was studied using the PRIMER software package. Abundances of the different species and copepodite stages were square root-transformed and used to derive a Bray Curtis similarity distances matrix between the different multinet samples and their depth layers. The resultant matrix was used to conduct a Multidimensional Scaling analysis (MDS), setting the 2D Stress limit to 0.15. Sample groupings with a similarity higher than 40 where then examined using a hierarchical cluster analysis and their characteristic species were found using the SIMPER procedure. Temperature, salinity, fluorescence, irradiance and nitrate+nitrite were normalised to create a semi-matrix of Euclidean distances and compare them with the zooplanktonic assemblage. Since salinity and density ($R_{S;\rho}=0.9999$) and nitrate+nitrite, phosphate and silicic acid ($R_{NO3+NO2;PO4}=0.7526$, $R_{NO3+NO2;Si(OH)4}=0.8183$, $R_{PO4;Si(OH)4}=0.7976$) were strongly correlated, only salinity and nitrate+nitrite were used in order to avoid collinearity. Finally, Bioenv and Stepwise analysis (BEST) was carried out to match both matrixes, testing the significance of the match with 999 random permutations of the rank correlation coefficient ρ.

Simple regression analysis was used to estimate both the relationship between the total mesozooplankton abundance and the abundance of its five main contributors *(C. finmarchicus, Microcalanus, Oithona spp., Copepoda nauplii, Oikopleura spp.)* and the relationship between the abundance of cod larvae and copepoda nauplii sampled in the 5 – 30 m layer. Choice of this layer was related to the sampling depth of the bongo net, in order to make the data comparable. Abundances in ind/m^3 were transformed into logarithmic form and the line equations and R^2 values were calculated for each regression.

Finally, Shannon Wiener (SW) Index was calculated in order to study the taxonomic diversity within and outside the patch. The different layers were divided according to the results from the MDS analysis.

3 Results

3.1 Physical and Biological Parameters

3.1.1 Hydrography

The two main currents dominating the area were identified by distinct temperature and salinity variations detected by the CTD. Lower salinities (< 35 psu.) at ca. 6°C were present at shallow depths extending down to ca. 100-150 m over the continental shelf, corresponding to the freshwater input advected from the nearby fjords by the NCC. However, the extension of this layer decreases in depth with distance from the coast and does not extend to off-shelf areas due

Transect S1

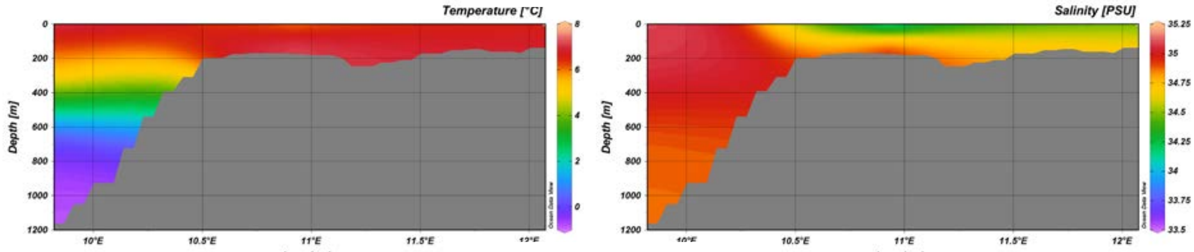

Transect S2

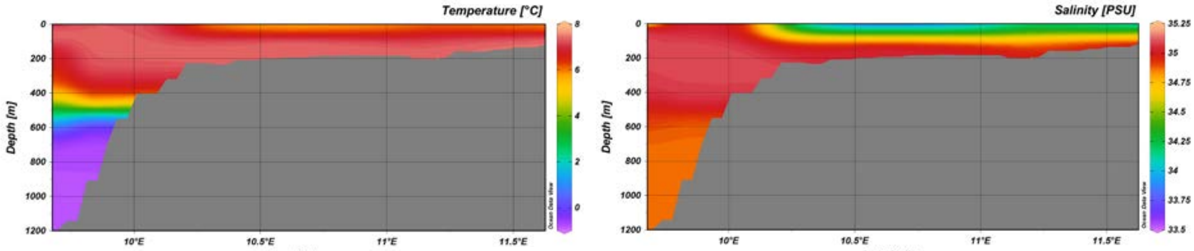

Transect S3

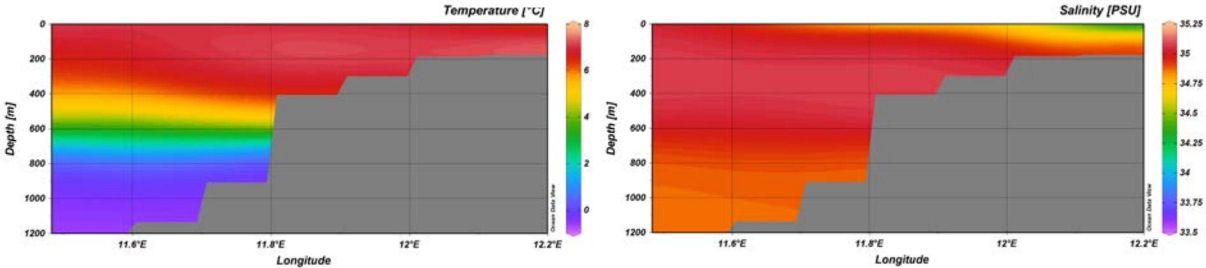

Transect S4

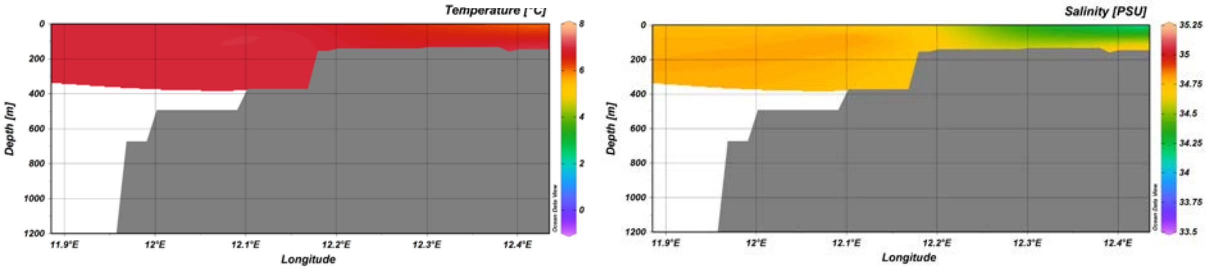

Figure 4: Temperature (left) and salinity (right) along the transects across the study area

to the strong density gradient caused by the AW, with T > 7°C and S > 35 psu driven into the area by the NAC. This is clearly visible in transects S1 and S2 *(Figure 4)*, as they extend further above the continental shelf. This warm and saline water input was observed down to ca. 600 m, mostly flowing along the shelf-break but also spreading onto the lower depths (> ca. 150 m) of the continental shelf. Below, as the influence of AW decreases, water temperatures decrease to minus degrees together with a reduction in salinity which is characteristic of the AIW.

By comparing the off-shelf profiles (St. 5, 8 & 9) we notice both temperature and salinity exhibit similar conditions for the first 400 m, with T > 7°C and S > 35 psu marking the border of the AW, although slightly lower temperatures were observed at station 9 *(Figure 5)*. However, this layer extends down to ca. 500 m in station 5 and ca. 600 m in stations 8 and 9, meaning the AW layer covers a greater fraction of the water column in the northern transects and thus the border with the AIW will be found deeper. Less variations are found between the shelf stations, where both T and S increase slightly with depth, indicating the transition between the freshwater influenced coastal water and the underlying AW. Nevertheless, temperature remains almost consistently low (< 6°C) at station 7, possibly due to its location further inshore, where the influence of the NCC is greater.

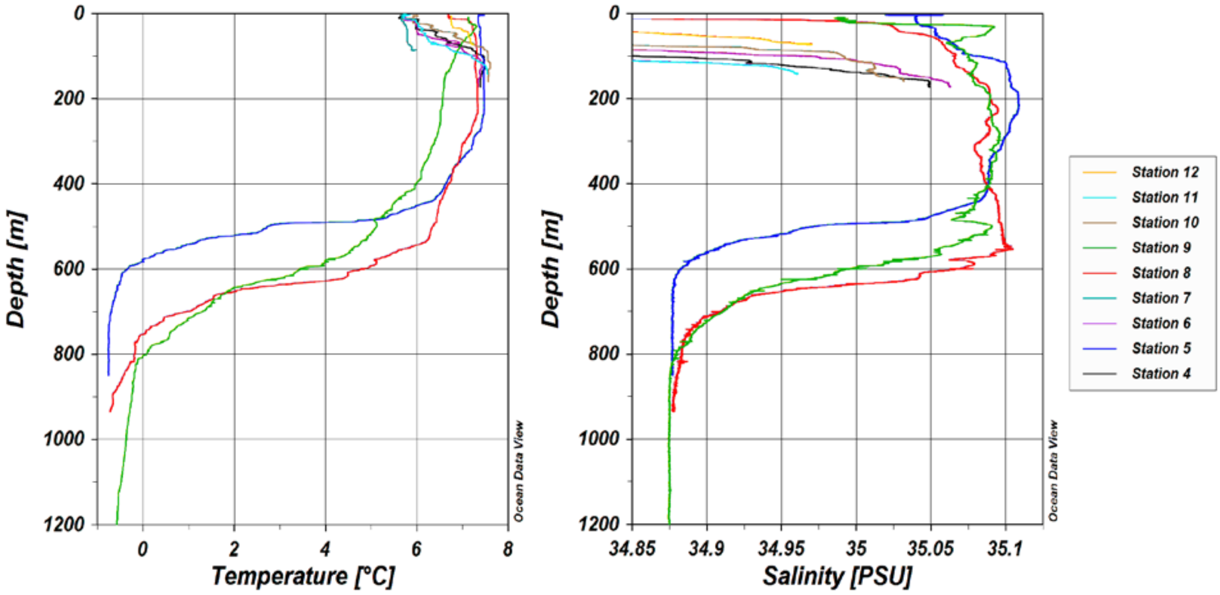

Figure 5: Temperature and salinity profiles for the different CTD deployments

3.1.2 Chlorophyll *a*

Water samples revealed generally low concentrations of chlorophyll *a* (<2 µg/L) in the area, with maximums occurring in the upper 15 m and decreasing with depth *(Figure 6)*. The low values (ca. 0.25 µg/L) remaining homogeneous throughout the water column at station 7 however do not respect this trend. Surprisingly, very high concentrations (ca. 5-6 µg/L), which triplicate the surface values of the other stations, were measured at station 8. Nevertheless, no clear relationship was found between the location of the station and the chlorophyll concentrations. Although slightly lower phaeophytin concentrations were found at some stations, values remained very similar to chlorophyll, following the same trend.

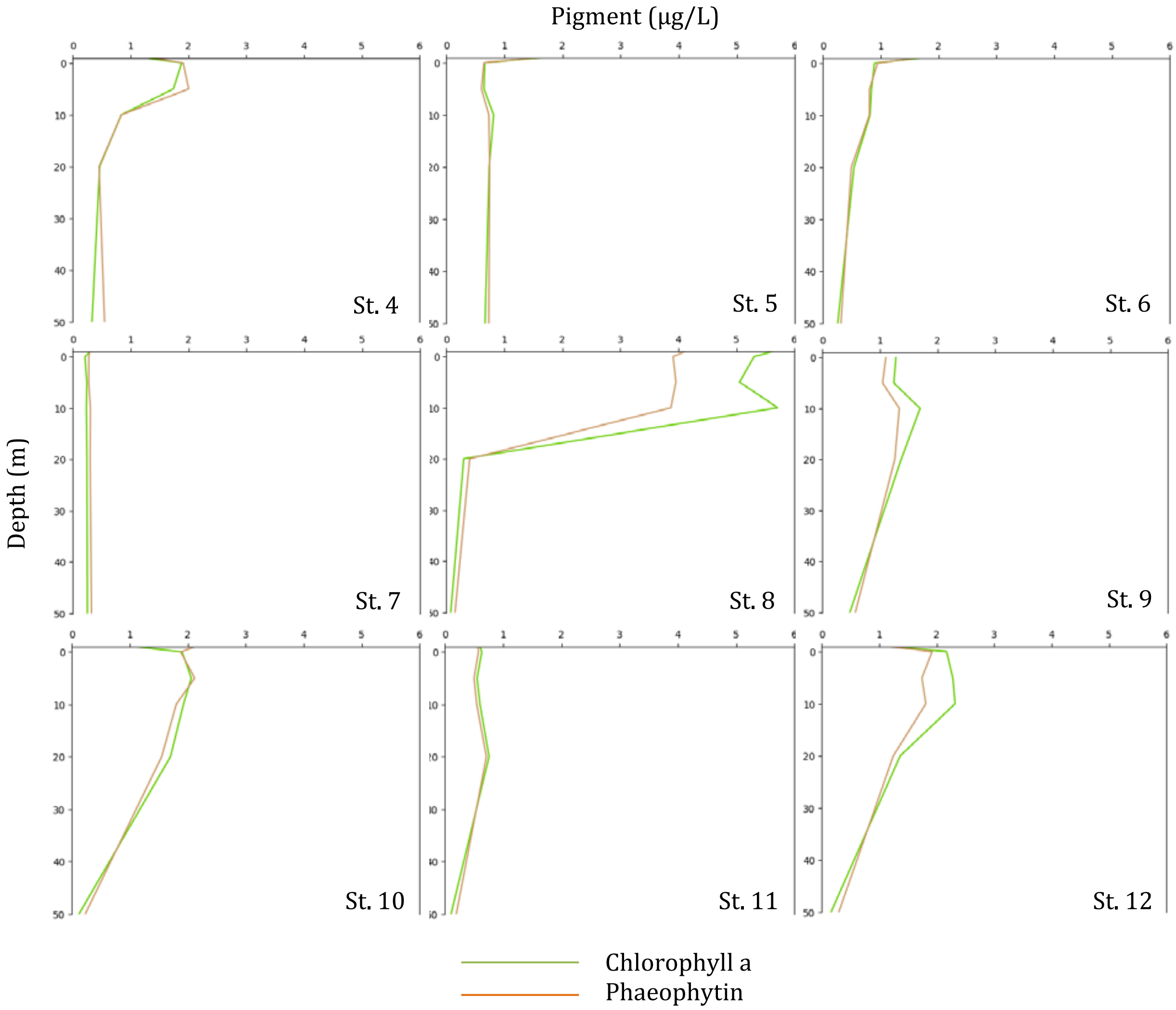

Figure 6: Chlorophyll *a* and phaeophytin profiles from the water samples taken along the transects

3.2 Acoustic Data

The acoustic data recorded by the EK 60 echosounder revealed a persistent high energy sound scattering layer (SSL) over the continental shelf, which ranged from the surface to a mean depth of 55.46 m *(Figures 7 to 10)*. By mapping the extension of the patch in the different transects *(Figure 18)* this trend is obvious. However, the depth range of the SSL decreases as we approach the continental slope. This tendency is clearly visible in the echograms corresponding to all transects except transect S3, where the SSL appears to maintain a similar depth range beyond the shelf-break *(Figure 9)*. Thus, the results show that high amounts of biomass are available for top predators over the entire shelf. Strong signals were detected by the 38 kHz frequency indicating the presence of larger organisms. The signal from zooplankton was thus classified by subtracting the 38 kHz signal from the 120 kHz signal. Deeper in the water column, a less dense epipelagic SSL is visible in the 38 kHz frequency at ca. 150 m over the shelf in the two southern transects.

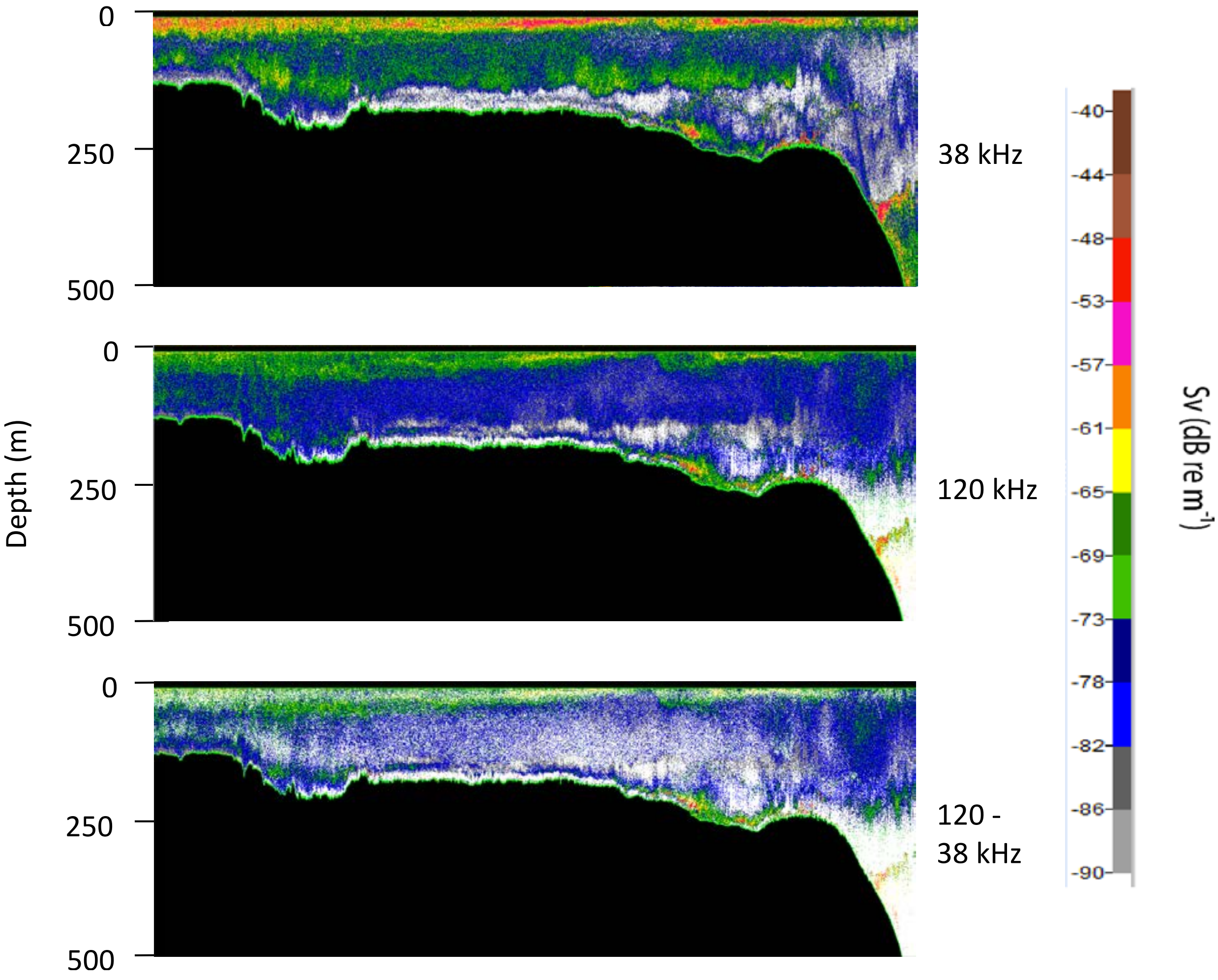

Figure 7: Volume backscattering strength echograms at 38, 120 and 120-38 kHz along transect S1

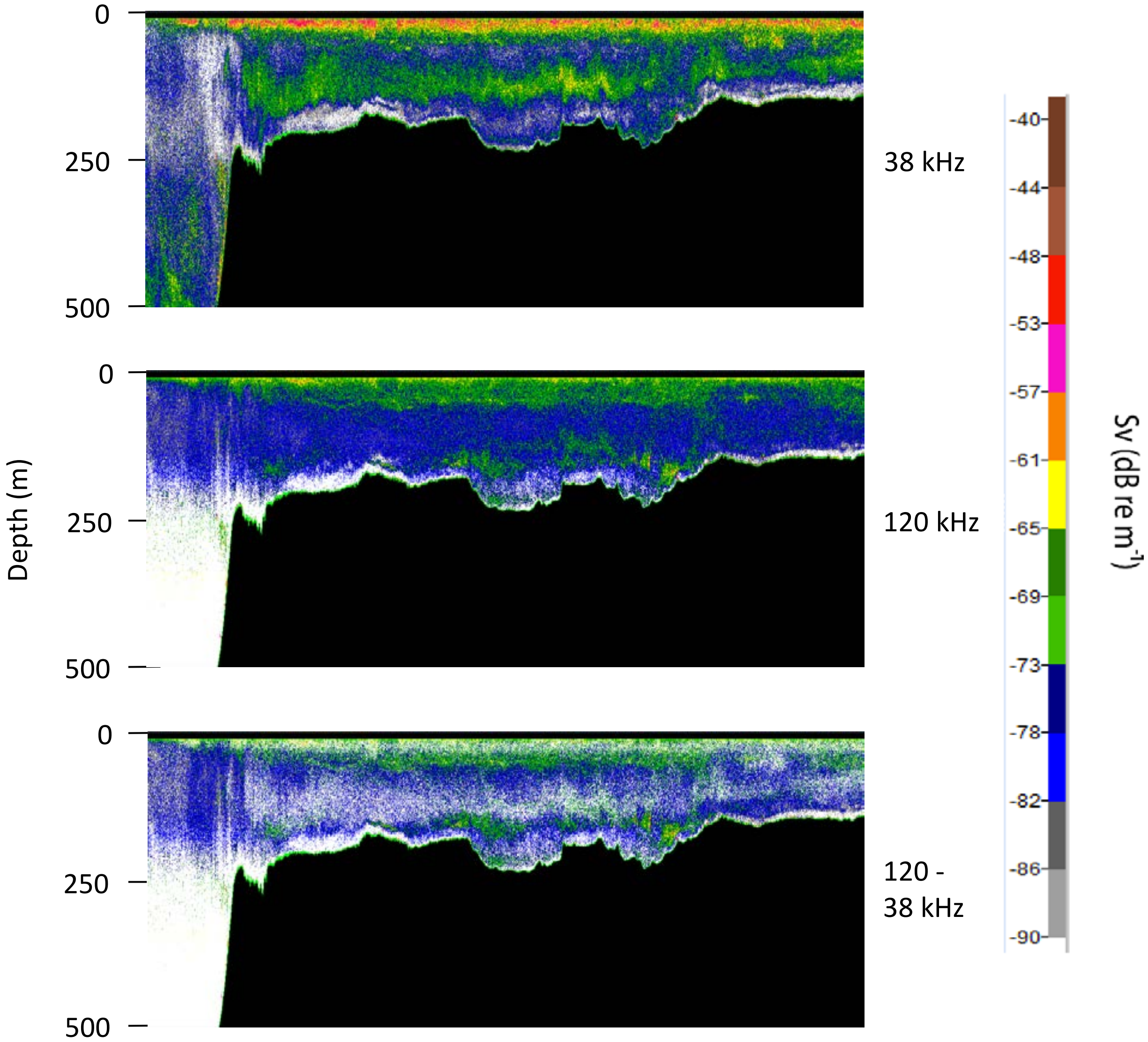

Figure 8: Volume backscattering strength echograms at 38, 120 and 120-38 kHz along transect S2

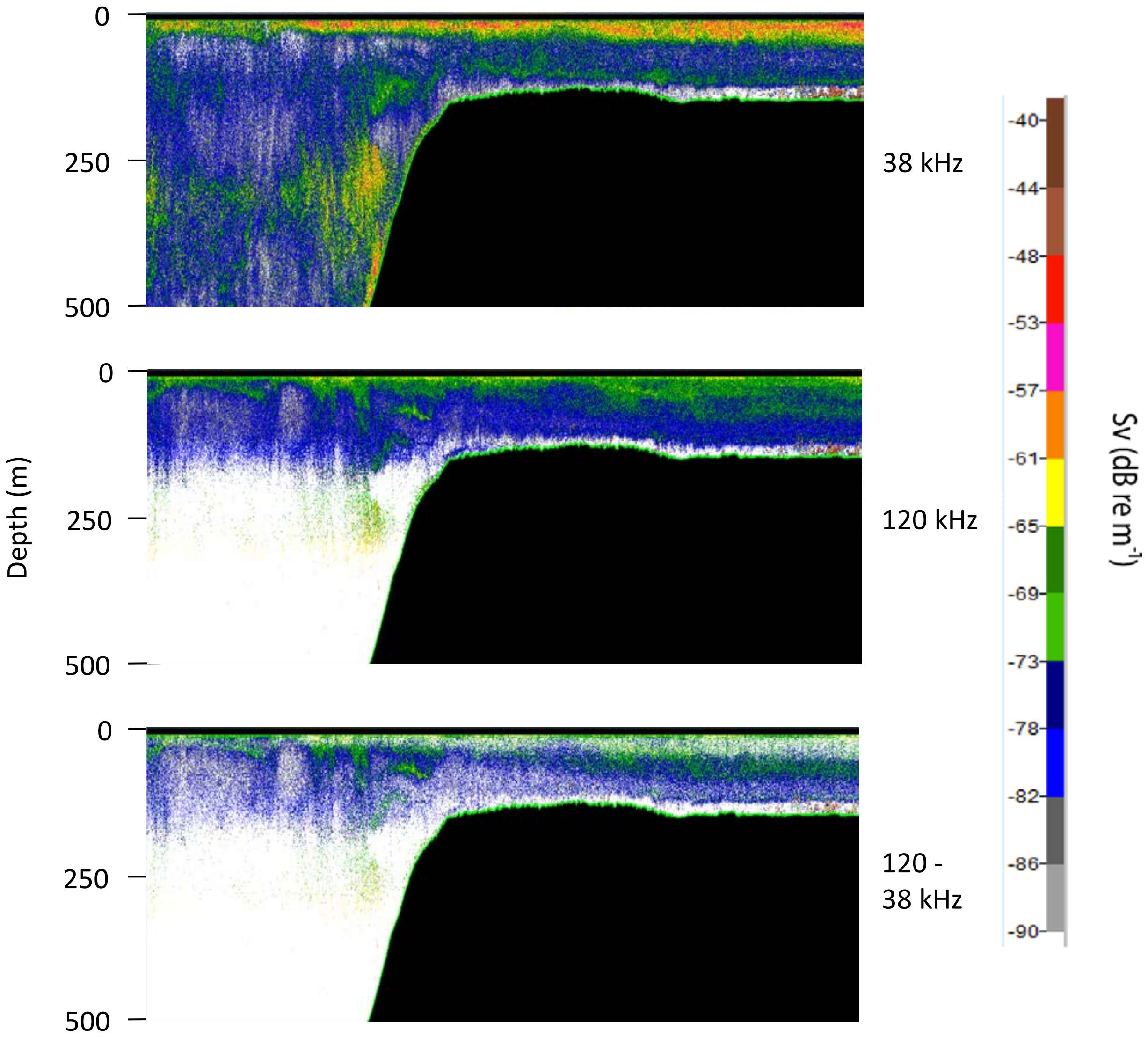

Figure 9: Volume backscattering strength echograms at 38, 120 and 120-38 kHz along transect S3

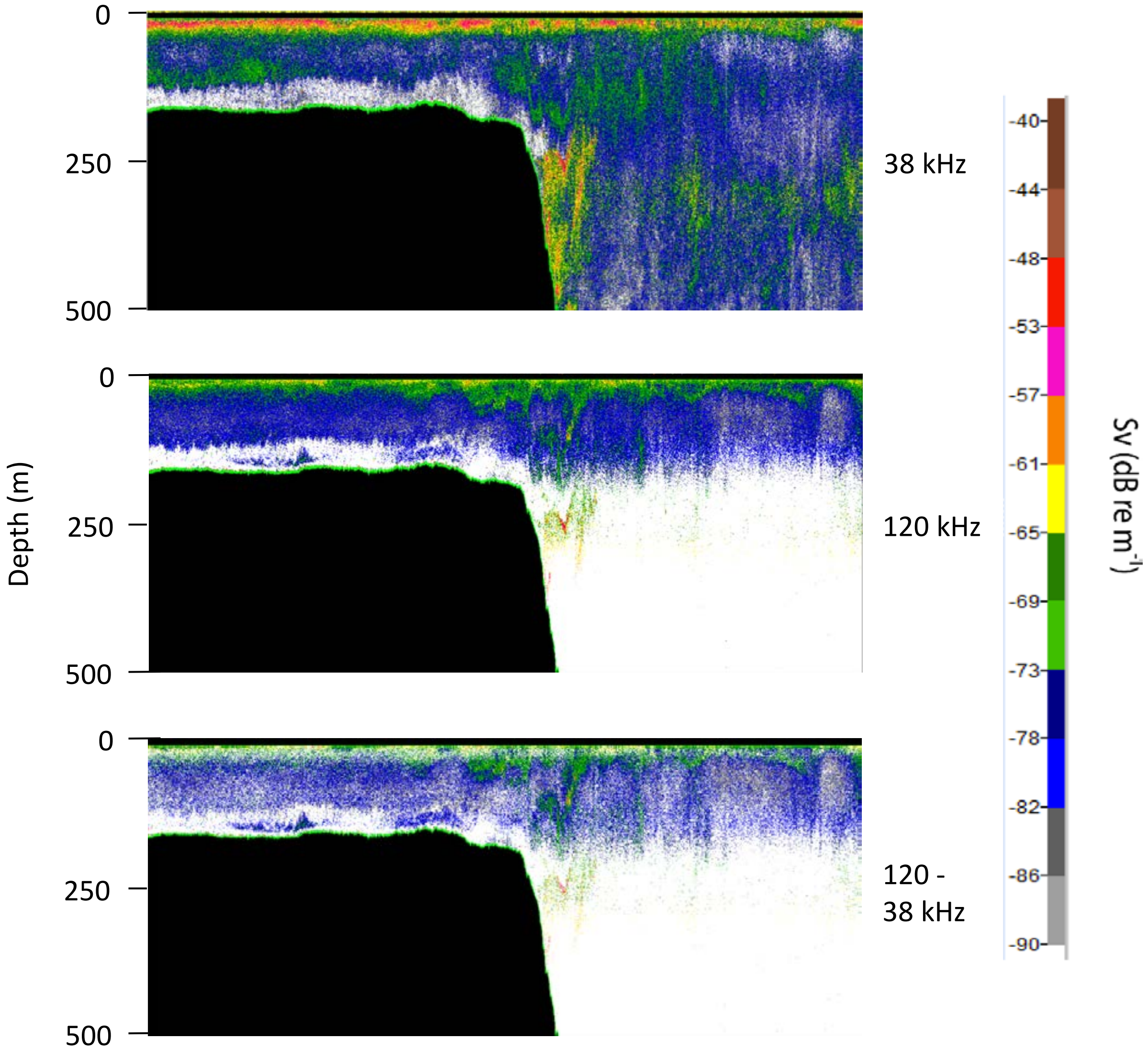

Figure 10: Volume backscattering strength echograms at 38, 120 and 120-38 kHz along transect S4

Acoustic species density calculations gave a mean value of 51229.32 ind/m^3 for the whole study area, with low SD (0.095) between the different transects, indicating near homogeneous distribution of organisms. MASD for species within the acoustic size detection range was highest for *C. finmarchicus* (41389.09 ind/m^3) and decreased significantly with increasing developmental stage ($p = 0.02$, $r^2 = 0.87$). However, we must take into account the MAD would have been notably higher if the first 12 m of the water column were noise-free and thus could have also been echointegrated, giving higher Sv values. Patch dimensions for the whole study area based on its extension along the 4 transects gave the following values: SA = 6501.90 Km^2, MD = 55.460 m, DSD = 16.809 m, V = 360595374 m^3. Acoustic calculation parameters can be consulted together with the full assemblage in the appendix.

3.3 Community Composition

The assemblage was strongly dominated by *C. finmarchicus* at almost all stations, which accounted for 80.5% of the community composition in the study area. This was especially remarkable in the southernmost transect where almost the whole community composition is represented by this species *(Figures 11 & 12)*. For instance, 98% of the organisms sampled at station 4 were *C. finmarchicus*. However, the general values are lower than 2150 ind/m^3 for off-shelf stations and higher than 3000 ind/m^3 for shelf stations. Within this trend, stations located in the northern transects were found to be more densely populated.

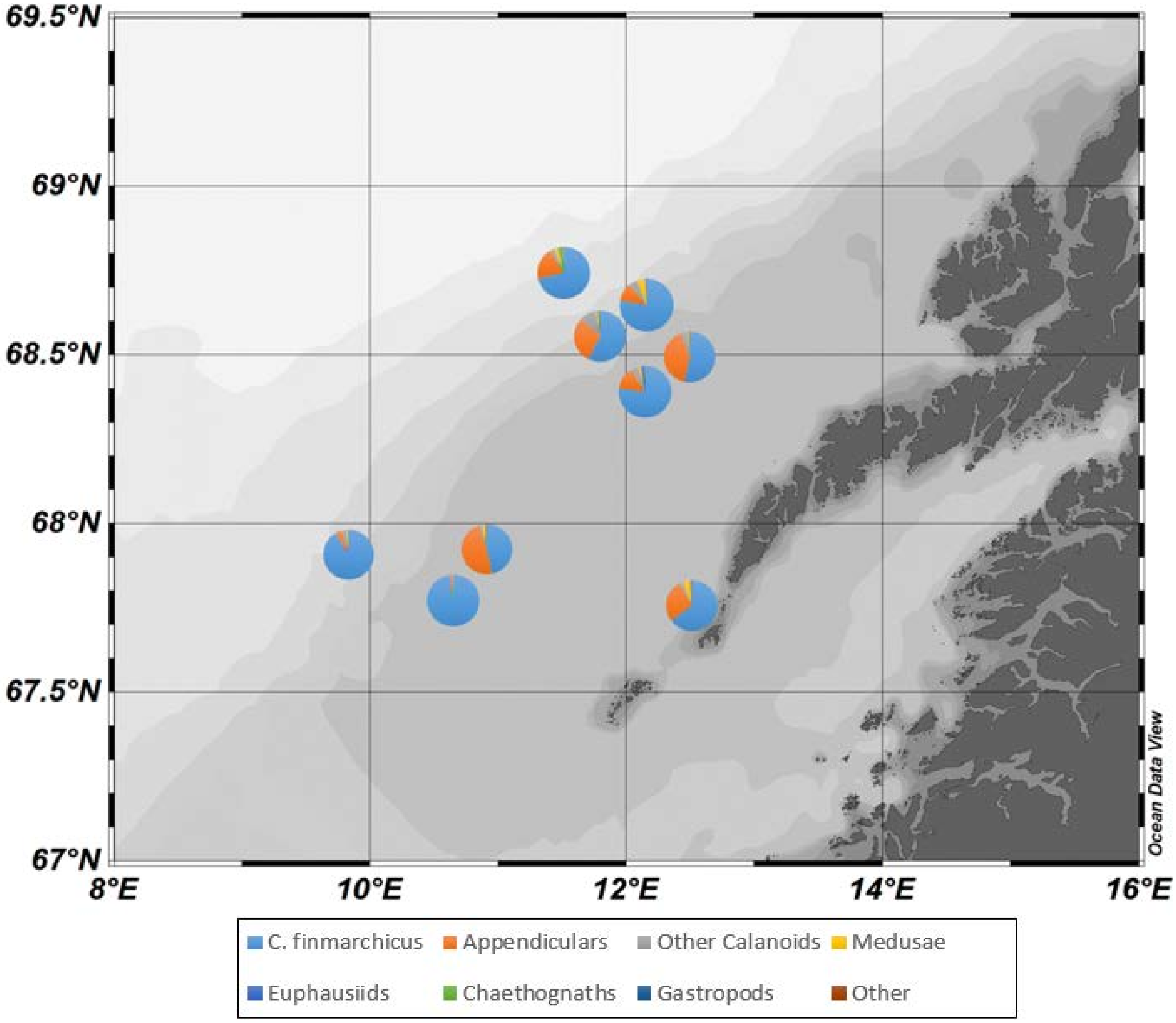

Figure 11: Relative abundance (ind/m^3) of C. finmarchicus and the main taxonomic groups within the acoustic detection size range expanded to the whole sampled water column at each multinet station

Appendiculars, mostly *Oikopleura dioica*, represent the next most abundant taxonomic group, contributing notably to the community as we move towards the north *(Figures 11 & 12)*. Except for transect S2, where low densities were found, high abundances ranging between 500 and

1500 ind/m^3 were observed at the different stations sampled by the multinet. Over 3000 ind/m^3 were sampled at station 6, making it the only station where the population of *C. finmarchicus* was overweighed by the abundance of *O. dioca*. Taxonomic diversity increased northwards as a result of higher abundances of other calanoids and medusa *(Figure 11)*.

Total abundance of organisms varies notably between the different stations, with significantly higher abundances registered on shelf stations than on off-shelf stations *(Figure 12)*. The ratio of organisms located in off-shelf stations versus on-shelf stations was found to be 1:6, meaning for each individual located off the shelf, 6 are found on the shelf. A clearly representative example of this is visible in transect S2, where station 4, located on the shelf, revealed the highest abundance of organisms in the study area (28611.11 ind/m^3), contrasting with station 5, located on the same transect but off-shelf, where the lowest density of individuals in the whole study area was observed (1265.88 ind/m^3) *(Figure 12)*. Multinet samples taken at different depths reveal higher abundances in surface waters which decrease with depth at most stations. The ratio of organisms located in the deepest sampled layer versus the shallowest sampled layer of all stations was found to be 1:11.3, meaning for each individual located in the lowermost layer, 11.3 are found in the uppermost layer. For instance, 20560.75 ind/m^3 were recorded in the upper 2 meters of the water column in station 4, contrasting with the 19.9 ind/m^3 present in the lowest depth strata (100-150 m) *(Figure 12)*. Nevertheless, how organized organisms are in the water column following this trend will vary from station to station. Once again, *C. finmarchicus* dominated the assemblage at most depths up to 100 m, followed by a notable contribution of appendicularians. However, below this depth it was mostly other calanoids that represented the greatest portion of the assemblage. Full assemblage can be consulted together with the acoustic calculation parameters in the appendix.

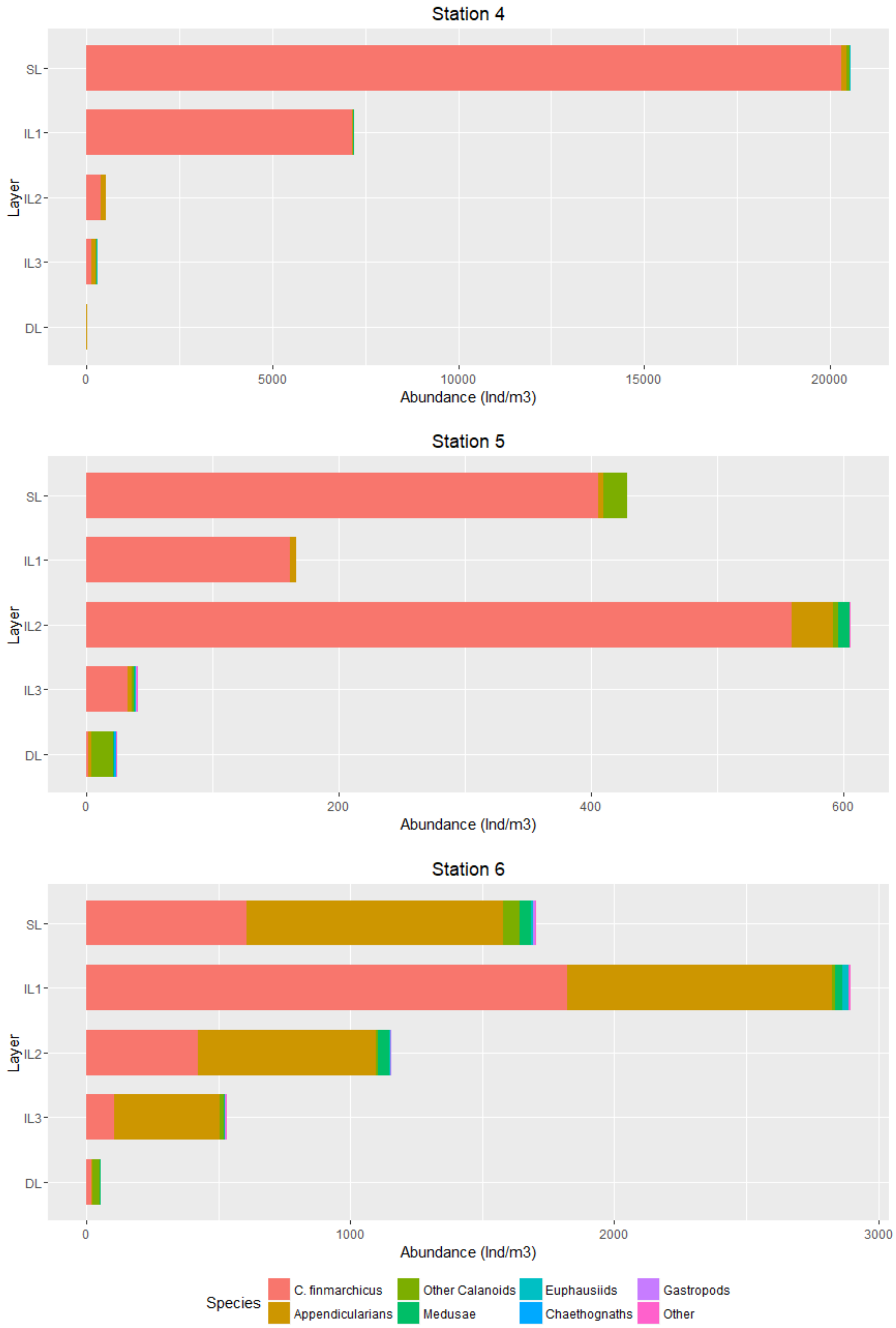
Station 4
SL
IL1
IL2
IL3
DL
Layer
0
5000
10000
15000
20000
Abundance (Ind/m3)
Station 5
SL
IL1
IL2
IL3
DL
Layer
0
200
400
600
Abundance (Ind/m3)
Station 6
SL
IL1
IL2
IL3
DL
Layer
0
1000
2000
3000
Abundance (Ind/m3)
Species
C. finmarchicus
Appendicularians
Other Calanoids
Medusae
Euphausiids
Chaethognaths
Gastropods
Other

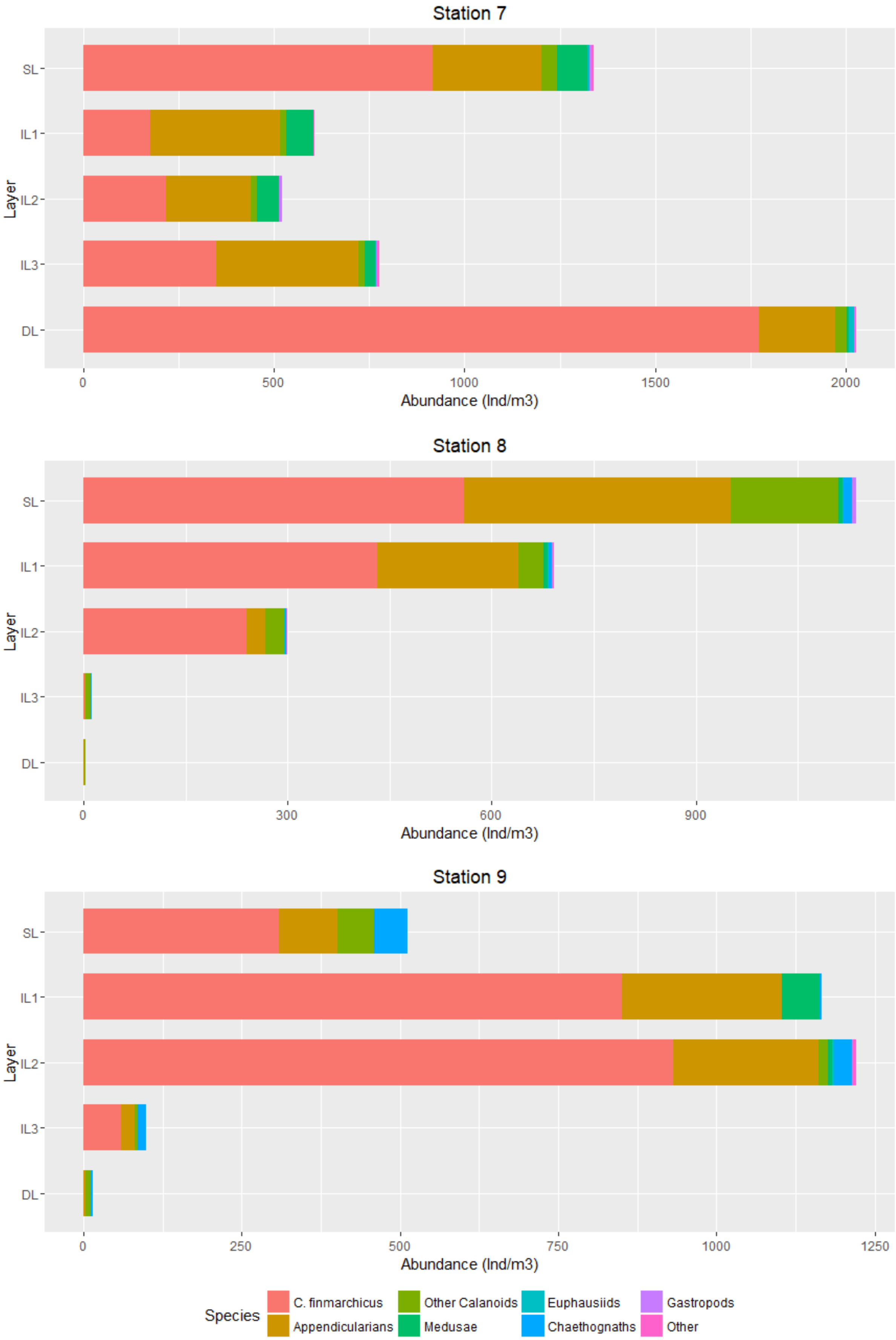
Station 7
Layer
SL
IL1
IL2
IL3
DL
0
500
1000
1500
2000
Abundance (Ind/m3)
Station 8
Layer
SL
IL1
IL2
IL3
DL
0
300
600
900
Abundance (Ind/m3)
Station 9
Layer
SL
IL1
IL2
IL3
DL
0
250
500
750
1000
1250
Abundance (Ind/m3)
Species
C. finmarchicus
Appendicularians
Other Calanoids
Medusae
Euphausiids
Chaethognaths
Gastropods
Other

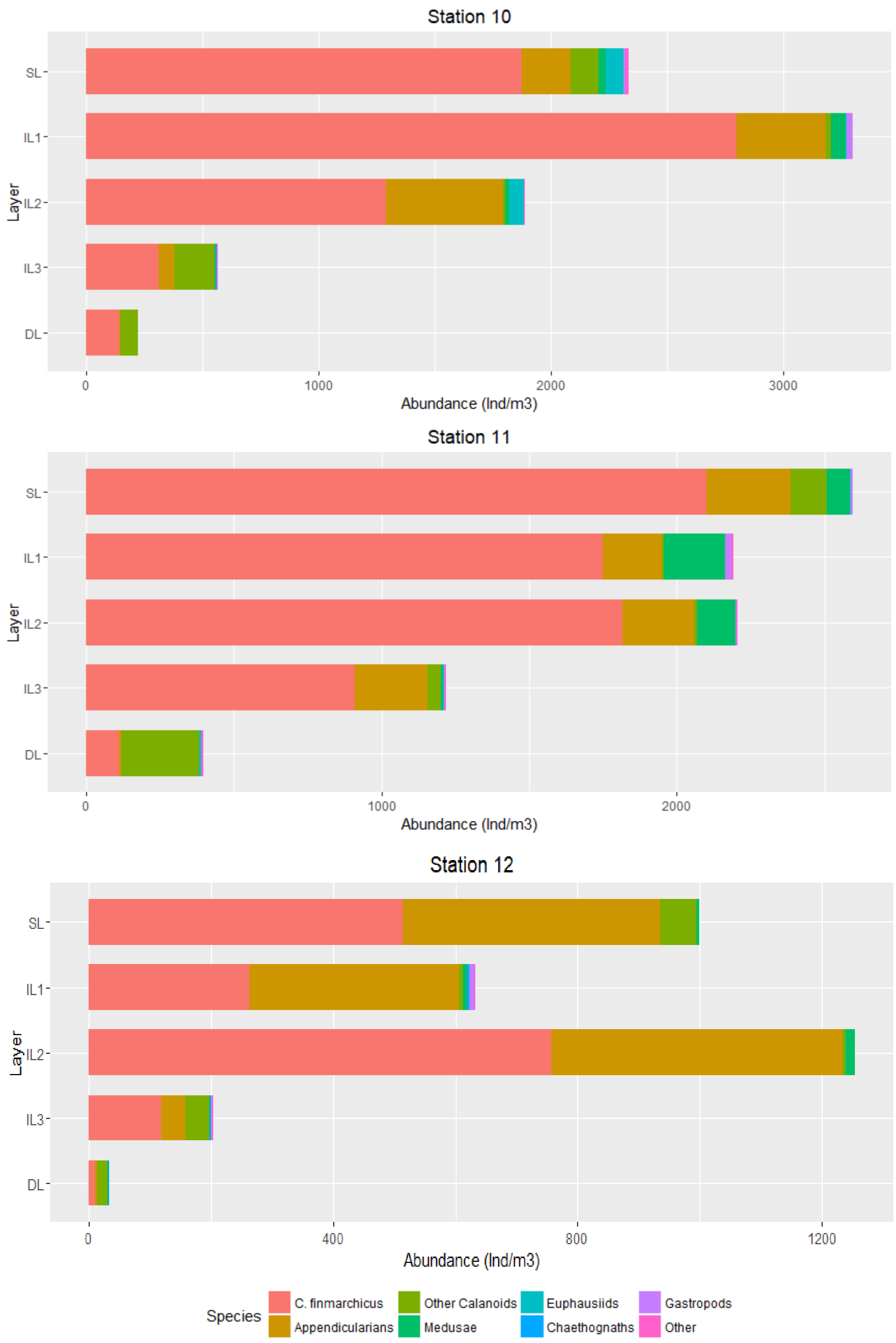

Figure 12: Abundance (ind/m^3) of *C. finmarchicus* and the main taxonomic groups at the sampled depth strata for a size range corresponding to the organisms detected with acoustics.

The multivariate analysis revealed three distinct sample groups, according to the composition of their zooplankton assemblages *(Figure 13)*. Group A comprised the largest amount of samples, representing a community composed mainly by copepoda species such as *C. finmarchicus* or *O. Similis* together with high numbers of nauplii. These remained in the trophogeneous upper layer, which extends throughout the top 100 m of shelf waters and the top 30 m of off shelf waters. Group B gathers samples taken in the lower part of the water column over the shelf (>100 m) and from 30 to 100 m off the shelf. It is dominated by *Microcalanus* and an increasing population of *Metridia spp.* and *Oithona atlantica*, which differentiates it from group A. Finally, group C covers the lower depths of off shelf stations, characterized by higher abundances of *Metridia longa* and ostracods. Thus, we can identify a trend displaying similar species found deeper in the water column on the shelf than off the shelf.

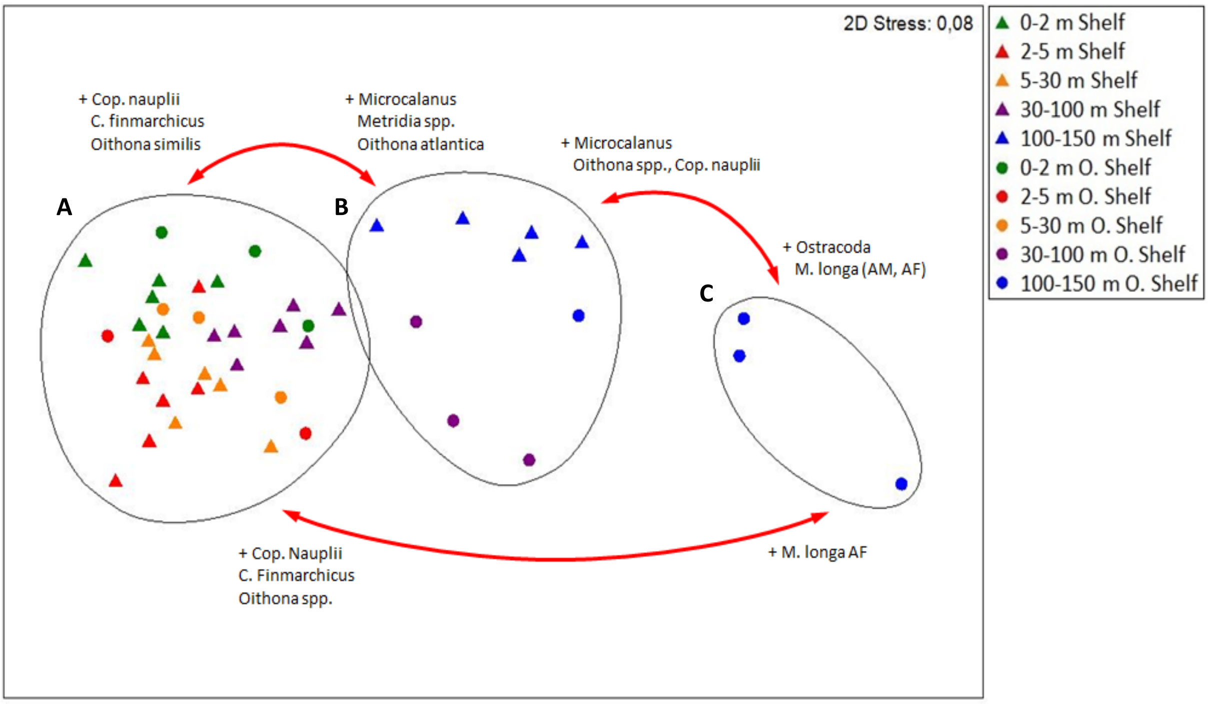

Figure 13: Results of the multivariate analyses. The MDS is represented with different symbols for sampling layer and location, and the different sample groups with a higher similarity than 40 (A,B & C) are sorrounded by a continuous line. The main species contributing to the different groups are specified

The BEST analysis revealed a subset comprising temperature and nitrate-nitrite represented the best match between the physical-biological parameters of the water column and the zooplanktonic assemblage, explaining 61.9% of the variance in zooplankton composition. Both variables correlated well with each other, with positive correlations ($r^2 = 0.894$) over the shelf. Although positive correlations can also be found within the upper 30 m at some off-shelf stations, lower depths displayed very low temperatures, meaning a negative correlation ($r^2 =$

0.809) will result if the whole temperature profile is taken into account. However, both variables correlated negatively with the abundances of the main zooplanktonic species, since they increase with depth while the highest abundances are found at surface.

Although generally low, the Shannon Wiener Index varied markedly between stations and depth layers, ranging from 0.24 to 1.249 *(Figure 14)*. Higher diversity was found in the upper layer above the shelf (e.g. St. 11) than off-shelf stations, where lower layers (e.g. St. 9) were more diverse. This means diversity decreased with depth over the shelf and increased with depth off the shelf. However, station 12 contradicts this trend, possibly because of the shallower depth range sampled (0 - 465 m) compared to other off-shelf stations.

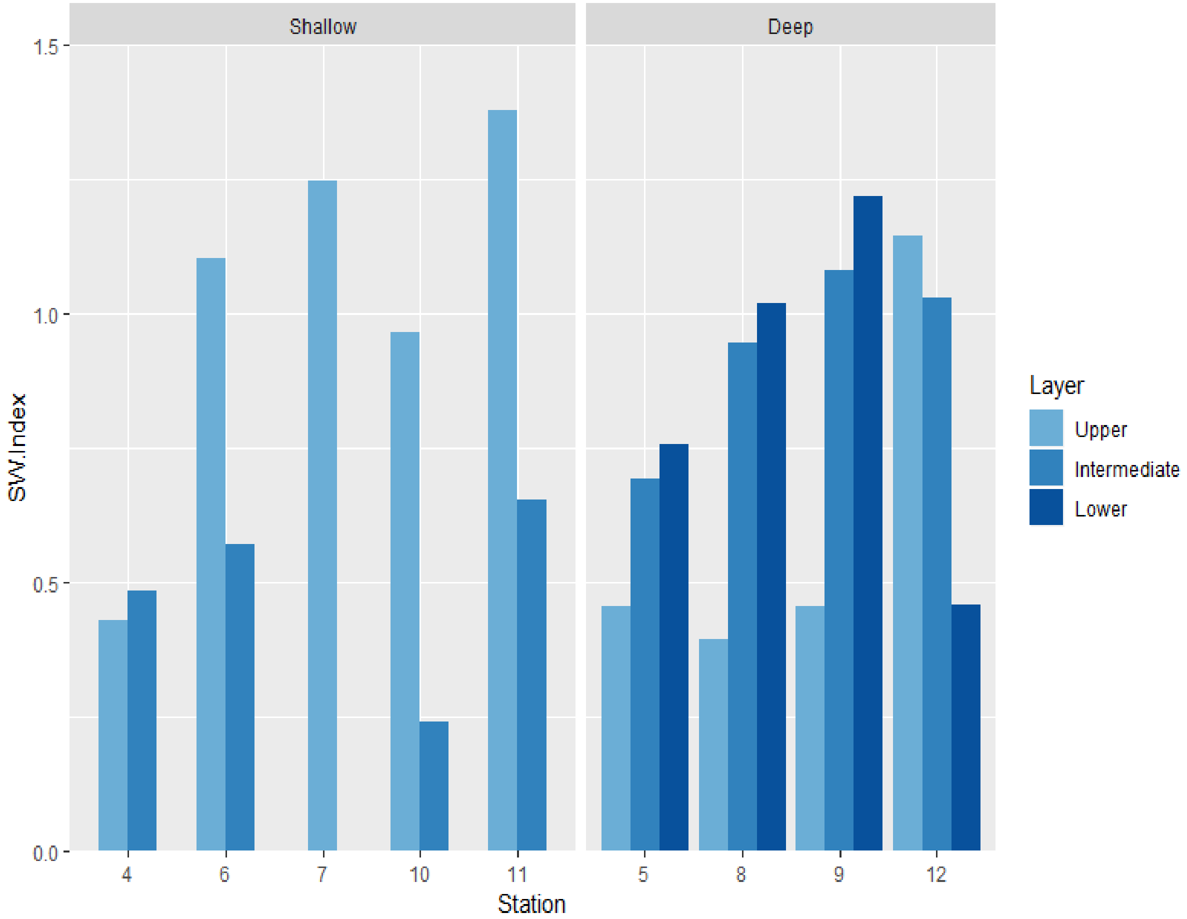

Figure 14: Shannon Wiener Index for the different stations divided into Upper layer (<100 m shelf, <30 m off shelf), Intermediate layer (100-150 m shelf, 30-100 m off shelf) and Lower Layer (>100 m off shelf)

Significant correlation between the total zooplankton abundance and its main contributors was only found for *C. finmarchicus (Figure 15)*. Linear regression analysis for this species revealed strong dependency of total abundance values on *C. finmarchicus* concentrations ($p = 1.08e-05$, $r^2 = 0.946$). Although not significant, all other species groupings exhibited positive correlations with a more gradual slope except for Chaetognaths, which decrease with increasing total abundance.

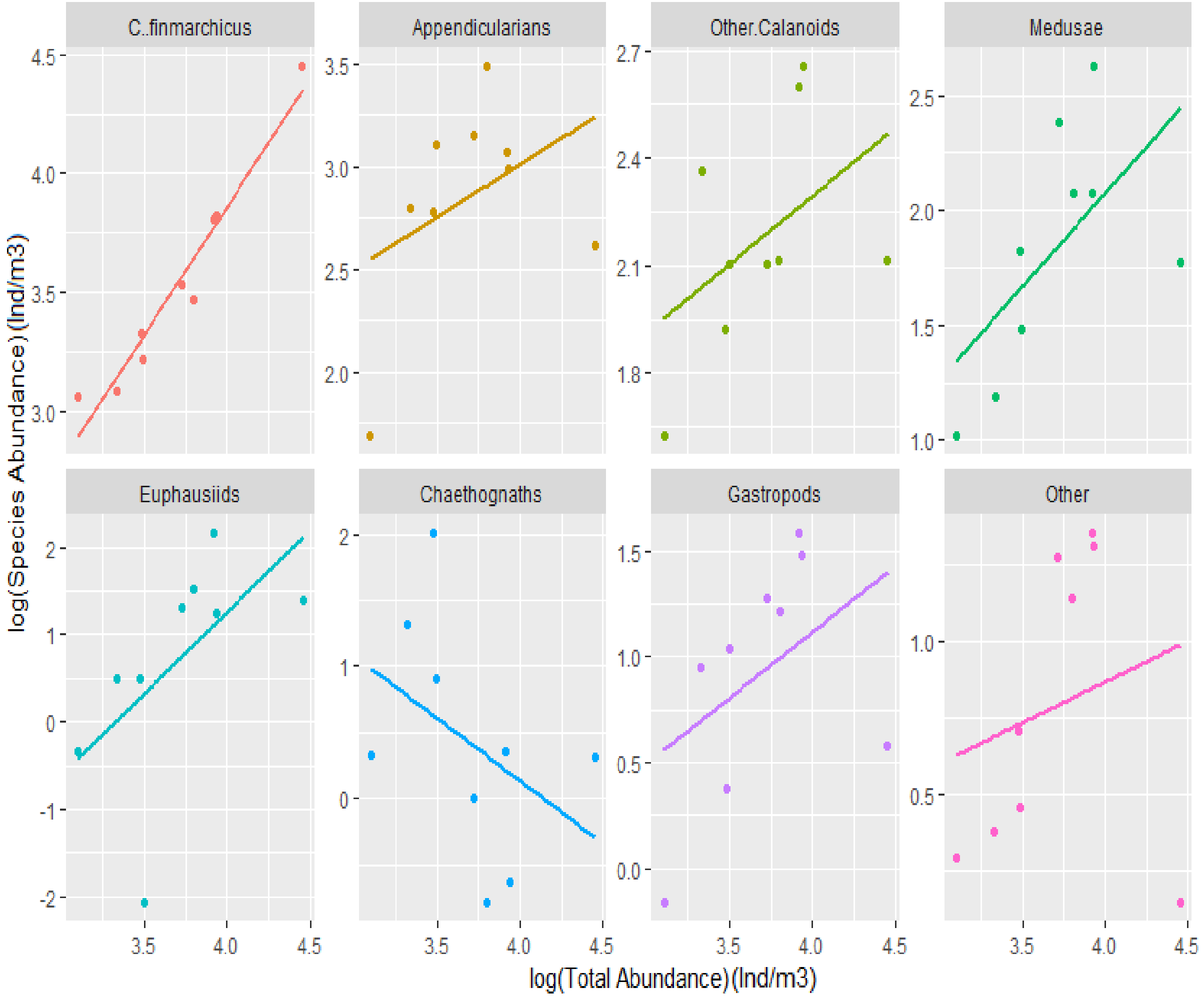

Figure 15: Simple regression analysis between the total zooplankton abundance, *C. finmarchicus* and the main taxonomic groups

Focusing on *C. finmarchicus*, developmental stage analysis of this species revealed the study area's population was generally in an intermediate stage, being CIII by far the dominating stage *(Figure 16)*. Younger organisms, generally CIII and younger, concentrated in shallower waters up to 100 m on the shelf, while deeper waters were generally dominated by CIV and older organisms, with a remarkable CV population. However, off the shelf older stages start to dominate from 30 m instead of 100 m. Thus, it is generally the deeper off-shelf stations that present the highest abundances of higher developmental stages compared to the shallower shelf stations, dominated by younger organisms. Nonetheless, we must take into account CV and CIV individuals were also found in high numbers at shallow depths, but they were outnumbered by the high abundances of lower developmental stages, resulting in a lower stage index for the overall population. Furthermore, although lower densities of adult stages were recorded, adult females dominated over adult males at most stations.

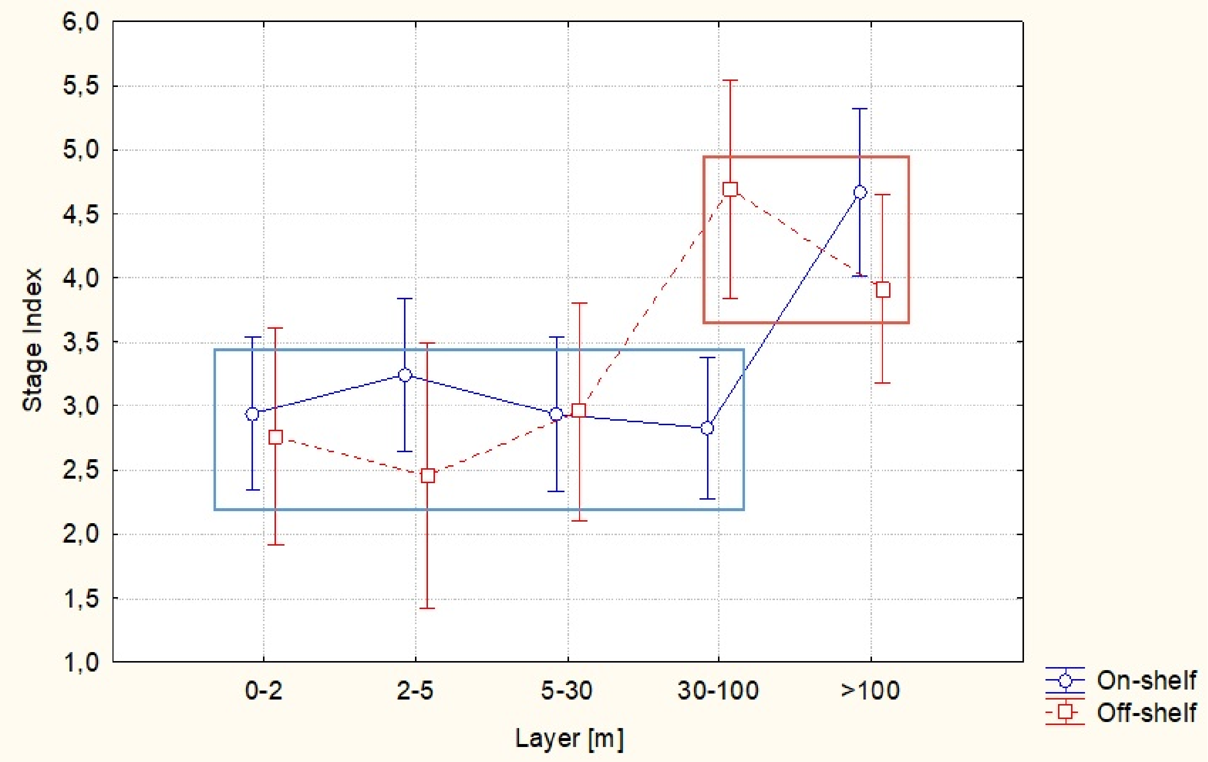

Figure 16: *Calanus* stage index mean and standard deviation at each sampled layer on and off the shelf. The blue box represents those samples taken in the NCC layer and the red box those taken in the AW layer

Bongo net sampling confirmed the presence of Atlantic Cod *(Gadus morhua)* larvae, a well-known predator of copepod egg and nauplii, in the study area. Due to the timing of the study, the larvae were still in a low developmental stage. Higher numbers of this species were found at shelf stations, being the most abundant at St. 7 (0.11 ind/m^3), compared to off-shelf stations, being less abundant at St. 8 (0.00013 ind/m^3) *(Figure 19)*. This gives a ratio of 1:18.1, meaning for each individual found off the shelf, 18.1 are found over the continental shelf. This matches with the highest concentrations of copepod nauplii, where significantly contrasting abundances were found on and off-shelf. A representative example of such disparity is found in transect 3, were 2364.9 ind/m^3 were sampled at St. 10, located on the shelf, compared to only 14.4 ind/m^3 at St. 8, located off the shelf. Simple linear regression analysis revealed a marginally significant positive correlation between their abundances ($p = 0.08$, $r^2 = 0.482$) *(Figure 17)*.

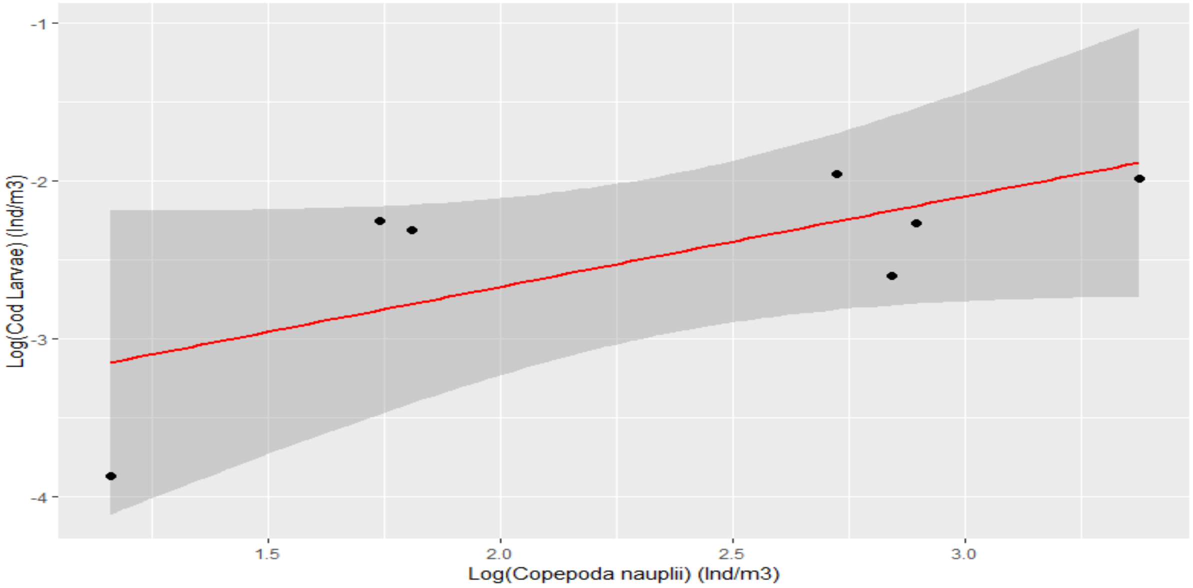

Figure 17: Simple regression analysis between cod larvae and copepoda nauplii abundance in the 5 – 30 m layer. Shaded area encloses 95% interval

4 Discussion

4.1 Advantages and Limitations of Acoustic-Trawl Surveys

A variety of methods such as Laser Optical Plankton Counters (LOPCs), Video Plankton Recorders (VPRs) or water pumping have been used by previous studies to document zooplankton patchiness. However, this thesis focused on results obtained through combining acoustic data and net sampling. Acoustic data visualized live on-board provided a continuous three-dimensional picture of the backscatter throughout the water column, allowing targeted deployment of net samples in biologically-defined depth strata. This combination enabled a high spatial resolution provided by the acoustics, essential for targeting large patches in the horizontal scale, and high taxonomic resolution of the patch composition provided by net samples. However, the exclusive use of sound to definitively identify aquatic organisms is unfortunately not possible because the amount of energy reflected, echo shapes and maximum amplitudes of the signal vary among successive returns from the same animal. The amount of sound energy returned from a target is dependent on the choice and configuration of hardware, water characteristics and location, composition, and behaviour of detected targets (Horne, 2000). This means active acoustic systems can be very useful for rapid data acquisition and processing particle abundance and size, but unfortunately they lack information on the taxonomic composition of the community (Gallager et al., 2016). Therefore, deployment of net samplers along the acoustic transects was necessary to ground truth the acoustic signal. This allowed the identification of the different species, enabling the estimation of the composition, structure and density of potential zooplankton patches together with the total relative biomass and abundance of the targeted species in the study area.

In most studies, zooplankton abundance and distribution are assessed by net sampling, which inconveniently provides discrete data in space and time. Additionally, zooplankton, particularly macrozooplankton, is known to avoid nets (Fleminger and Clutter, 1965; Brinton, 1967; Debby et al., 2004; Lawson et al., 2008) because of both visual and mechanical disturbances (Fleminger and Clutter, 1965); this avoidance being higher when using smaller nets. Avoidance generally results in a systematic underestimation of macrozooplankton biomass if the sampling bias is ignored. However, acoustics allows a simultaneous collection of highly accurate qualitative and quantitative data on various communities of an ecosystem, from zooplankton to large predators, providing a comprehensive vision of their distribution. Therefore, one of the main motivations for the use of acoustics for this project was the possibility of sampling organisms that would otherwise be missed by net samplers, in order to resolve the distribution of *Calanus* patches in greater spatial detail.

Nonetheless, the quality of our data was constrained by severe spatio-temporal limitations arising when mapping zooplankton abundance and distribution from ships. The area covered was limited to the vessel's track and differences in the timing between stations and transects could have affected the results. In addition, ships disturb the surrounding environment physically, meaning the location of organisms in the water column could have been altered, especially near the surface. In this sense, using autonomous platforms equipped with the adequate instrumentation such as unmanned ocean gliders could provide higher quality data when targeting zooplankton patches.

4.2 Patch dimensions and morphology

This study provides a high resolution, three-dimensional view of zooplankton patchiness in the Lofoten-Vesterålen region. The results show a persistent SSL over the entire continental shelf. However, as we move towards the shelf-break, the density of the SSL slowly decreases and stops above off-shelf areas. We conclude that the patch extends across the continental shelf until it reaches the shelf-break, where it dissipates. However, the lack of cruise time only enabled the completion of 4 transects, meaning the dimensions in the latitudinal axis are only roughly mapped.

When determining patch location, dimensions and morphology from the available transects, various possibilities were contemplated *(Figure 18)*. Despite the lack of acoustic data between northern and southern transects which would allow a more accurate approach of the patch, an idea of the patch parameters can be obtained from the available data. One of the possibilities is the presence of two different and independent patches, located one within the area of the southern transects and the other one within the area of the northern transects. A different interpretation of these results would be that it was the same patch located further north due to the influence of the north-flowing currents present in the area. Nonetheless, similarity between the acoustic species density calculations for the different transects indicated near homogeneous distribution of organisms, suggesting the whole area could be covered by the same aggregation. This possibility involves a large patch extending between the northernmost and southernmost transects, consisting of SA = 6501.90 Km^2, MD = 55.460 m, DSD = 16.809 m, V = 360595374 m^3 and a MASD of 51229.32 ind/m^3 *(Figure 18).* These results compared well with the ground data, proving a realistic representation of the community. Combining these results with other data sets and previous literature (e.g., Pinca and Huntley, 2000; Wishner et al., 1988; Basedow et al., 2018) we can conclude a large patch expanding across the continental shelf and northwards along the shelf break is the most probable patch morphology.

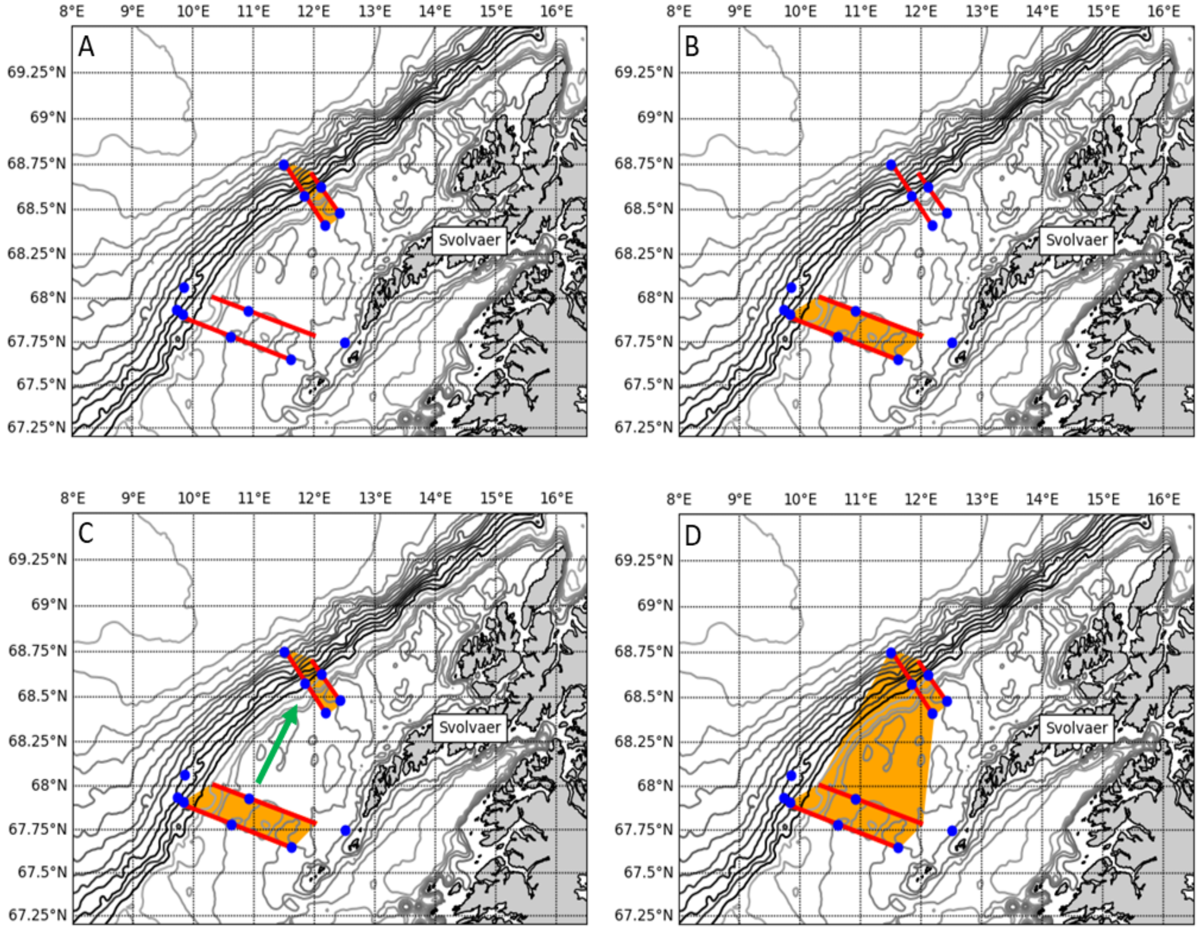

Figure 18: Plots of the different possible patch formations in the study area. A and B represent the first possibility, C represents the second possibility and D the third and most probable possibility, on which we will focus. The shaded area is the area covered by the patch, the red lines represent the extension of the patch in the different transects and the blue dots locate the different stations

Similar macro-scale zooplankton patches (>100 km) have been previously detected by Pinca and Huntley (2000). Wishner et al (1988) detected an extensive, nearly continuous surface layer of *C. finmarchicus* occupying an area over 2500 km^2 using a 200 kHz acoustic system. Although there is a large unsampled area between transect S1 and transect S3, there is a series of determining factors that support this conclusion. Firstly, no clear hydrographic differences have been spotted as we moved north along the continental shelf, indicating environmental continuity. Patterns in temperature and salinity remained relatively homogeneous between northern and southern transects compared to the notable differences spotted between off-shelf and shelf stations. This suggests a large continuous patch instead of two separate patches, as no hydrographic or topographic features that could potentially interrupt the northward flow of organisms were observed. Likewise, acoustic species density calculations gave very similar values for the different transects, meaning patch composition remained highly homogeneous throughout the study area and thus suggesting it involves the same aggregation of organisms.

Satellite images of the study area revealed very strong red pixels extend from the southern end of Vestfjord and along the edge of the continental shelf, corresponding to areas where high concentrations of *C. finmarchicus* were found in surface waters *(Figure 19)*. However, these pixels are not visible beyond the shelf-break. Basedow et al (2019) confirmed such pixels could be attributed to *C. finmarchicus'* astaxanthin pigment, suggesting a large and continuous patch morphology restricted to shelf areas extending south from Vestfjorden and covering the whole continental shelf as we move northwards.

Although a long-term study would be necessary to accurately analyse the persistence of such patch, the satellite images reflect little variation from the general patch morphology over 5 consecutive days *(Figure 19)*. Furthermore, despite the difference in time between southern and northern transects, no major variations were found in the net samples, acoustic transects or species density calculations. This suggests a stable and consistent patch structure, similar to the one followed by Cushing and Tungate (1963) in the North Sea. During this study, they tracked the southerly drift of a *C. finmarchicus* aggregation which had already formed by the start of the observations and was still recognizable after 66 days, when the study ended. Thus, persistence of large patches in off-shore waters can probably be frequently measured in weeks or months.

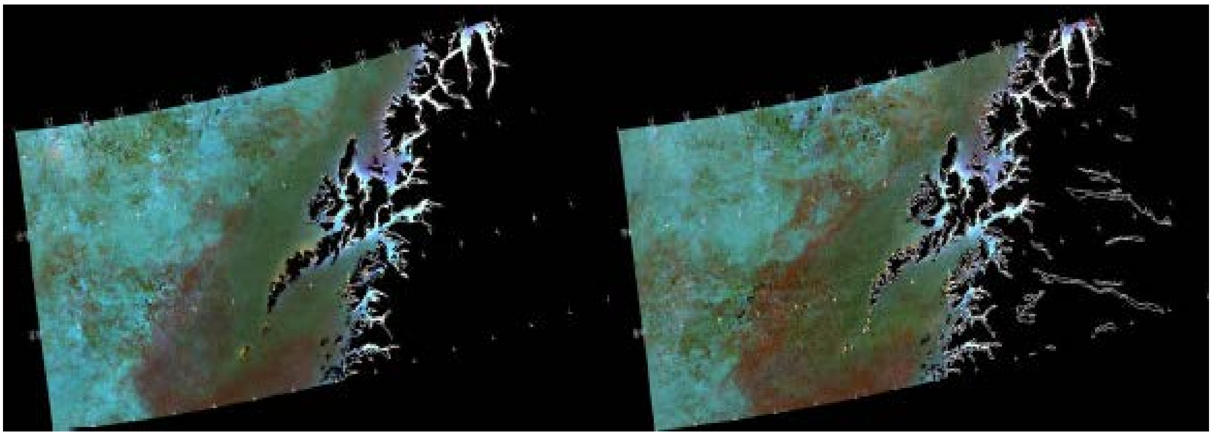

Figure 19: VIIRS RGB images from (left to right) 29th April and 3rd May 2017. Images processed and distributed by NEODAAS.

Moving on to the vertical extent of the patch, the location of the patch in the water column extended from the surface to a mean depth of 55.46 m according to the acoustic data *(Figures 7 to 10)*. However, stratified net samples found the highest concentrations were in the top 30

m. This could result from the variating depth of the aggregation along the transects, possibly influenced by both physical and biological drivers, which will be discussed later. What was clearly observed in both data sources were very high abundances at surface which decreased with depth. Although acoustic data from a hull-mounted echosounder can only be trusted below ca. 12 m, meaning the most abundant layers at surface were excluded, a considerable difference was obtained in the MAD within the patch compared to outside the patch. This agrees with the multinet samples taken at different depths, which showed much higher abundances within the patch layer, and with the Sv values obtained by performing echointegration, which revealed higher signals were detected by the EK60 within the same layer.

This difference is remarkably notable for *C. finmarchicus*, which has the highest MASD of the assemblage and doubled it within the aggregation compared to outside it. Mean vertical acoustic profiles taken by Ritcher (1985b) revealed surface horizontal patches of zooplankton 4- to 15-fold above background population densities in deeper waters. Moreover, dense surface aggregations, <15 m deep, of the similar species *Calanus pacificus*, were observed along a tidal front during spring by Gómez-Gutiérrez et al (2007). Thus, surface aggregations of zooplankton seem to be attractive for these organisms, and possible drivers shall be further studied.

Statistical analysis revealed similar abundances in the top 30 m of the water column along the whole transects. However, significant reductions in abundance within this top layer were detected over the shelf, while off the shelf no major variations were observed. Below 30 m the situation is the opposite. A steady decrease in abundance occurs off the shelf, while a significant decline from the surface layers is not seen over the shelf until below 100 m. This contributes to the higher abundances observed over the shelf in comparison to off-shelf waters. A possible reason for this could be the coastal water layer being confined to shallower depths as we move off-shelf, meaning AW water is found further up in the water column. Since most organisms seem to be restricted to the coastal water layer, this would negatively affect the abundance of copepods at shallower depths off the shelf compared to over the shelf, where the warm and saline water input is found deeper, allowing organisms to remain in the coastal water layer for a greater fraction of the water column. Nonetheless, this pattern must be related to copepod behaviour, since no significant variations were found for other organisms. However, since copepods dominate the assemblage, this tendency will have a notable influence in the general patch shape.

4.3 Species Assemblage within the Patch

Patch composition analysis revealed a highly diverse assemblage consisting of 52 different taxa. This accounts for 64% of the number of sampled species throughout the whole water column being found within the patch limits. Multispecies aggregations are not uncommon and have been previously observed in both oceanic (Haury and Wiebe, 1982) and shallow areas (Wishner et al., 1988). This type of grouping is usually considered a special case of the predator-induced group, where the aggregation of different species provides additional benefits for the whole group. For instance, differences in sensory capabilities among the species involved in the aggregation could provide a more complete predator detection system for the group as a whole. Thus, such mutualisms could improve the defensive mechanisms of the group, reducing predation risk for all group members. However, since the species found were mostly zooplankters, it seems they accumulate at surface in order to exploit the high primary productivity during the spring bloom instead of aggregating as a defensive reaction to predation risk. Moreover, multispecies aggregations witnessed by previous studies (e.g., Wishner et al., 1988) consist mainly of a few species, meaning a high fraction of the organisms found in the net samples could be just drifting by and not actually forming part of the patch.

Species-specific depth preferences derived in statistically definite communities at diverse depths. This appeared to be strongly related to the vertical stratification of the water column and the occurrence of phytoplankton. MDS analysis spotted different groupings of samples according to the composition of their zooplankton assemblages. Copepoda nauplii, *C. finmarchicus* and *O. similis* were broadly distributed species, but remained primarily in the upper layer. However, *Microcalanus* was found below the thermocline in the intermediate layer, which suggests detritus is the main source of food of this species instead of living algal cells (Krause and Trahms, 1982). This contrasts with the previously mentioned copepods, which directly depended on the highest concentrations of phytoplankton located in the surface layer. Thus, the differences in their location in the water column proves physical properties are not the only driver of plankton patchiness, but also feeding strategies (Krause and Trahms, 1982). Finally the deeper layer was characterized by higher abundances of *Metridia spp.*, especially *M. longa*, which is characterized as a bathypelagic species but has been observed closer to the surface in Arctic waters (Daase et al., 2008). Our results are in agreement with the findings by Bollens et al (1993) and Daase et al (2008). These studies proposed *Metridia spp.* possibly exhibit greater avoidance of the well-lit surface layer than *Calanus* because the former can be more susceptible to predation by planktivorous fish. Similar to the case of *Microcalanus*, *Metridia spp.* are considered omnivorous species which might therefore be more flexible when selecting their vertical position, since they are less dependent on the phytoplankton bloom.

However, their distribution in the water column varied from shelf to off shelf waters. MDS analysis revealed that similar groupings of organisms were found shallower off the shelf than over the shelf. Cross-shelf distribution of the major zooplankton species is conditioned by their depth, salinity and temperature preferences, vertical migration behaviour and by cross-shelf water-mass distribution, movement and exchange (Coyle and Pinchuk, 2005). The fresh, nutrient-rich water layer driven by the NCC to the study area extended deeper over the shelf than off the shelf, where the AW was present higher in the water column. Thus, organisms such as *C. finmarchicus* or Copepoda nauplii that are restricted to the top, colder layer will be found shallower off the shelf, followed by those with preferred conditions within the underlying AW layer such as *Metridia spp.*. These organisms are probably transported onshore with bottom waters by the intrusion of AW over the shelf displayed in the CTD transects, settling in the bottom layer above the shelf.

Species variations with depth displayed by the MDS analysis affected the species diversity assessed through the SW Index. This was consistent in showing lower diversity in surface waters than deep waters off the shelf and opposite conditions over the shelf, tendency that has been reported else-where (e.g., Mann and Lazier, 1996; Kosobokova and Hopcroft, 2010) Off-shelf, higher diversity at depth was driven mostly by other calanoids such as *Metridia spp.* and *Microcalanus*, species' known to have lower depth preferences (e.g., Daase et al., 2008), together with the widely distributed cyclopoid *Oithona spp.*. On the other hand, higher diversity at surface over the shelf, which displayed the highest overall SW Indeces, was linked to herbivorous copepods such as *C. finmarchicus* and their nauplii, appendicularians and their associated predators such as *Centropages spp.* or *Temora longicornis*, and the pelagic larval forms of other taxa such as polychaetes, echinoderms and bryozoans.

Despite the notable biodiversity of the area, *C. finmarchicus* clearly dominated the assemblage, accounting for 80.5 % of the whole community. Very similar results were obtained by Aarflot et al. (2017), who showed that *Calanus* species constituted 80% of the mesozooplankton biomass in all regions of the Barents Sea. Furthermore, comparable prevailing abundances of *C. finmarchicus* were found by Wishner et al (1988), who observed a 20 times higher concentration factor for this species than for other copepods within a large scale zooplankton patch. The strong correlation revealed by the simple regression analysis denoted the heavy influence of *C. finmarchicus* in the total zooplankton abundance, meaning patch formation will be strongly dependant on this zooplankter. Thus, variations in its concentrations together with *Calanus*-specific behaviour will play an important role in the structuring and maintenance of the patch (Wishner et al., 1988).

Stage index analysis disclosed younger *C. finmarchicus* life stages were in general associated to shallower waters (< 30/100 m) compared to older stages, which although present in the upper layers in minor numbers, dominated deeper in the water column (> 30/100 m). This shows both generations are represented in the ecosystem. The new generation of organisms is already developed and is found grazing in surface waters, while individuals of the old generation are still migrating upwards from off-shelf overwintering depths. Similar results were obtained by Lamb and Peterson (2005), who found naupliar and early copepodite stages remained within the warm, phytoplankton-rich upper 20 m of the water column, but copepodite stages C3 and older settled at progressively deeper strata in the water column.

The ANOVA analysis unveiled significant difference between the distribution of development stages at shelf and off-shelf stations. Older stages appeared to dominate in shallower waters off the shelf than on the shelf, where they were not abundant until >150 m. This suggests the older stages are associated to the warmer AW mass, which is found higher in the water column off the continental shelf. However, the proximity of overwintering grounds to the study area could also play a role in the timing of the new generation development. Heath et al (2000a) defined proximity of overwintering habitats as one of the main determining factors of *C. finmarchicus* demography and productivity at a given site. In this sense, G0 individuals overwintering at shallower depths in nearby fjords such as Vestfjorden (Espinaase et al., 2016) could have started the reproductive season earlier over the shelf, leading to the numerous G1 generation encountered by this study in surface waters. On another hand, G0 individuals overwintering in deep off-shelf areas such as the Lofoten Basin may take longer to rise to shallow phytoplankton rich waters located over the shelf, developing their offspring later in the season. Furthermore, these individuals could be confined to the AW layer by the strong density gradient between the AW and the colder and less saline water from the NCC, which could act as a barrier and inhibit their expansion to shallower waters, thus delaying their offspring development. This population could be represented in the higher abundances of older developmental stages detected by this study off the shelf.

Kvile et al. (2014) studied the temperature effects on *C. finmarchicus* developmental stages in the Norwegian and Barents Sea. They found abundances of CIV−CV were strongly correlated with temperature in spring, and higher slope values were predicted in areas with generally higher abundances in the Norwegian Sea. If these organisms were members of the G1 generation, high abundances of older stages could be expected if higher temperatures anticipated the start of the bloom, as suggested by Johannesen et al. (2012). This would trigger an advanced abundance maximum of young stages which could propagate into an advanced peak of older stages due to the higher growth rates driven by the higher temperatures (Kvile et al., 2014). Nevertheless, the early timing of this survey suggests that most CV individuals encountered belonged to the G0 generation, since individuals of the G1 generation require a longer period of time from the start of the spring bloom to develop into CV stage.

The second most abundant taxonomic group in the community after *C. finmarchicus* was appendicularians, mostly *O. dioca*. No significant variations were found in their horizontal distribution, although surface waters reflected higher abundances. Aggregations of eggs and juveniles can be quite common at surface, since appendicularians are known to spawn in the first few meters of the water column. This opportunistic species has a quicker response than copepods to favourable conditions due to its fast growth rates, allowing them to be the first to take advantage of the spring bloom (Troedsson et al., 2002). This means high abundances found during this study are not surprising, even early in the season. Nonetheless, at 8 of the 9 stations they are outnumbered by slower growing copepods in the community. A possible driver of such situation was suggested by López-Urrutia et al (2004), who studied the active consumption of juvenile *O. dioica* by various calanoid copepod species. They confirmed species such as *Centropages typicus* or *Temora longicornis* predated on ca. 1 mm long *O. dioca*, meaning appendicularians could represent an extra step in the trophic chain. A negative relationship between appendicularians and the same species' was witnessed by Stibor et al (2004), suggesting appendicularians are under strong pressure from calanoid copepods.

Although the most abundant calanoid copepod, *C. finmarchicus*, is a herbivore species unlikely to affect the abundance of appendicularians, these calanoid copepods together with other omnivorous species such as *Metridia lucens* were observed by this study. However, they tend to alternate between herbivory and carnivory diets in relation to the availability of plant and animal food in the environment (Landry, 1981). Therefore, during the spring bloom, high phytoplankton concentrations are enough to satisfy the feeding requirements of calanoid copepods, resulting on a decreased predatory pressure on appendicularians (López-Urrutia et al., 2004). Thus, this could be a possible explanation for the high abundances of appendicularians found during phytoplankton blooms, like in the present study. Probably, when chlorophyll values decrease further in the season, appendicularians will become an alternative food source for the copepod population, resulting in a decrease in the larvacean density.

4.4 Physical drivers

Patterns of plankton patchiness in marine systems at mega- to macro-scales, as it appears to be our case, seem to be mostly linked to physical processes (Pinca and Huntley, 2000). One of the main reasons for this is zooplankton forms patches and not schools, since schools imply the ability to swim against any current by constantly moving (Mauchline, 1998). This is because, despite *C. finmarchicus* having one of the highest swimming speeds (1.23 mm/s) among calanoid copepods (Hardy and Bainbridge, 1954), they are known to be relatively weak horizontal swimmers (Mauchline, 1998). They perform upward and downward movement in loops or spirals, which involves hardly any horizontal movement (Mauchline, 1998), meaning they are left to drift with the ocean currents. Thus, in order to be distributed extensively over the continental shelf, they must be subject to physical drivers. This suggests that water masses acting as boundaries to zooplankton assemblages can be expected to a higher extent on less active organisms (Gallager et al., 2016).

The cyclonic gyres of the Irminger Sea and the southern Norwegian Sea, two major hydrographic features, have been described as the two centres of distribution of *C. finmarchicus* in the North Atlantic (Sundby, 2000). Replenishment of the local stocks from the gyre results in high abundances of this species in the regions bordering the Norwegian Sea gyre, such as the continental shelf and the fjords of western and northern Norway (Wiborg, 1954). This agrees with the high concentrations of *C. finmarchicus* detected by this study in the continental shelf off the coast of the Lofoten-Vesterålen archipelago.

The distribution of the aggregation being restricted to the continental shelf matches with the hydrography of the area, where the colder and less saline NCC is present over the continental shelf down to depths ranging from 100 to 150 m. This water mass becomes less dense as we move off-shore, until it meets the NAC, which drives AW into the study area. The highest concentration of organisms tends to be subject to the NCC, possibly due to its preferable conditions. The BEST analysis revealed a significant match between temperature and the zooplankton community, but this variable was negatively correlated with the abundance. This suggests that although organisms could benefit from faster growth rates in warmer waters, which would enable an earlier descent to overwintering depths in order to avoid predation, they prefer colder surface waters. A possible reason for this resides in the cold freshwater input, which tends to be nutrient rich and could thus be a source of high PP. However, since most organisms are believed to be advected to the study area either from the south following the NCC or from nearby fjords such as Vestfjorden, the high density gradient formed between the two currents could possibly act as an important mechanism to restrict cross-shelf water exchange throughout the year. This presents a barrier for the advection of organisms to off-shelf areas, forcing them to remain on the shelf. A similar distribution pattern where major taxonomic groups aggregated in patches at coarse scales because of their association with specific water masses of different origin and their associated temperature/density discontinuities was found over Georges banks by Gallager et al (2016). These results however disagree with those reported by Trudnowska et al (2016), who rejected any association between the distribution of large scale patches comprising mostly *Calanus* species and any specific hydrographic or hydrodynamic feature.

Nevertheless, variations regarding the location of organisms in the water column exist between stations. These variations could be related to the different weather conditions experimented along the cruise track. At stations where conditions were stable, the layering of organisms was much more defined and organized, with high concentrations at surface which decrease as we gain depth (e.g. St. 4). A comparable study by Pinca and Huntley (2000) proved similar vertical structures, where the most superficial layer had the highest concentration of organisms. On the other hand, at stations where the weather picked up, organisms were spread throughout the whole water column following no clear, stratified pattern (e.g. St. 9). We thereby suggest that calm conditions enable more stable layering, since organisms can select their preferred location in the water column. Meanwhile, rougher weather conditions result in the mixing of the water column, meaning relatively weak swimmers such as *C. finmarchicus* have difficulties for settling within their preferred location. Therefore, such organisms tend to concentrate in areas of high vertical stability (Gallager et al., 2016). This is not only visible in the net data, but also by looking at the acoustic transect 3 where the off-shelf station 9 is located and where we can observe how the SSL continues off-shore along the shelf-break. This means that weather induced mixing of the water column could weaken the previously described “barrier” between the two different currents.

Another relation between the distribution of organisms and the weather conditions in the area concerns the timing of the bloom. Before the phytoplankton spring bloom can start, there must be a stabilization of the water column over deep and well-mixed areas (Sverdrup, 1953). Over the shelf, this is achieved by light coastal water lying on top of AW, causing a marked salinity stratification. Moreover, Menden-Deuer (2012) observed high nutrient concentrations in areas where phytoplankton aggregations occurred and suggested water masses associated with patches remained isolated for several days without mixing with waters at other depths. Thus, stable conditions are required for phytoplankton blooms to occur.

This agrees with our results from the CTD transects, which demonstrated that the less saline NCC was present over the whole shelf in the upper 100/150 m, with the AW lying underneath. Moreover, models and ocean satellite data suggest that the temperature increase recorded in the Barents Sea between 1998 and 2006 has resulted in a progressively earlier start of the spring bloom (Johannesen et al., 2012), meaning temperature could be positively associated with the observed early bloom start. Hence, stable and warm conditions observed in the study area could have anticipated the start of the spring bloom by increasing the vertical stability of the upper layer and the subsequent reduction in depth of the upper mixed layer. This could have triggered the early migration of grazer species such as *C. finmarchicus* from overwintering depths to shelf areas. An early start of the bloom could explain the high concentrations of CIII and CIV stages of *C. finmarchicus* present in the study area already at the time of the study, revealing a well established new generation population.

Proximity to an overwintering centre has been suggested to be the main prerequisite for high abundances of *C. finmarchicus* (Heath et al., 2000a), meaning overwintering on the northern Norwegian shelf can contribute significantly to sustain a *C. finmarchicus* population in shelf waters during the period of first feeding for cod larvae (Espinasse et al, 2016). However, abundances of *C. finmarchicus* CV in shelf areas during winter rarely exceed 2000 ind./m^2 (Halvorsen et al., 2003), suggesting they are too shallow to provide an overwintering habitat. This implies that as *C. finmarchicus* ascends from its overwintering habitat to spawn in spring, it is conducted onto shelf areas by surface circulation (Backhaus et al., 1994). Thus, the high abundances of *C. finmarchicus* found by this study are assumed to be advected to the continental shelf from other overwintering populations, such as those overwintering in the Lofoten Basin at 800–1200 m depth, in local fjord environments located close to the study area, or in the southern Norwegian Sea.

Therefore, although acoustic data and satellite images suggest a consistent patch, we must take into account that it is not constantly the same organisms that form the aggregation, as they are continually being advected northwards by the prevailing currents. A study by Koszalka et al (2011), concluded that the highest current speeds in the Norwegian Sea were found along the Norwegian coast both for the NAC and the NCC, with speeds of ca. 30 cm/s. A strong NCC is usually located closer to the coast and water masses near the entrance of fjords, advecting more organisms at higher speeds directly to the north-western coast of the Lofoten Islands both from southern areas and nearby fjords. This tells us we are not facing a resident population but a population in constant northward drift, where organisms within the patch drift northwards at high speeds. A model designed by Ådlandsvik and Sundby (1994) showed particles released in the Lofoten area were distributed northwards by the north-flowing currents along the coast and had reached as far as Nordkappbanken in only 30 days. However, organisms are constantly being advected by the NCC from overwintering areas, aggregating over the whole shallow continental shelf outside the Lofoten-Vesterålen islands and thus replenishing the population of *C. finmarchicus* in the area.

Nonetheless, the origin of *C.finmarchicus* is still unclear. Since growth rates of zooplankton are slow compared to the time scale of mixing, patches are likely to represent organisms which developed at a different location and have been subject to a physically driven re-distribution. Many studies (e.g., Halvorsen et al., 2003) propose the spring invasion of the North Norwegian shelf is partly the result of the northward advection of *C. finmarchicus* from the overwintering sites in the southern part of the Norwegian Sea. This could be easily expected, since most of the copepods flowing northwards with the NAC and NCC are probably transported up to regions located further north. Heath and Jonasdottir (1999) observed abundances in the Faroe-Shetland Channel were more than adequate to account for the observed abundances in the northern North Sea. They thereby suggested that a fraction of the copepods ascending from overwintering areas close to the Faroe Islands may reach as far as the Lofoten-Vesterålen shelf areas during spring and summer, becoming a source of the increasing Lofoten basin overwintering population.

Hydrographic variations over the shelf, possibly explained by differing levels of freshwater discharge and wind conditions, are likely to have an effect on the plankton distribution (Skarðhamar et al., 2007). The copepod community overwintering in the Lofoten basin could be advected to shelf areas by the eastbound replenishing movement of AW at depth onto the shelf occurring when the less saline surface water is spread by the NCC (Pedersen et al., 2001). This cross-shelf process can be seen in our salinity profiles, where AW flowing along the slope penetrates onto shelf areas below the lighter coastal water, suggesting this process as a primary source of intra-annual variability in the *Calanus* stock of the Lofoten-Vesterålen shelf.

Moreover, patchiness of both phyto and zooplankton in the study area could originate from plumes of plankton-rich fjord water trapped in eddies over the banks. Similarly, cod eggs spawned inside Vestfjorden and developing larvae are eventually transported out of the fjord system and drift northwards into the Barents Sea with the prevailing currents. This occurs in strong NCC conditions, since when this current is stronger, it flows closer to the coast, advecting water masses near the entrance of fjords directly to the northwestern coast of the Lofoten Islands (Espinasee et al., 2016). Thus, in addition to the overwintering stocks further south and in the Lofoten basin, *Calanus* overwintering on the shelf and in nearby fjords may contribute to the high concentrations found by this study in the Lofoten-Vesterålen shelf areas. This highlights the importance of the NCC in the aggregation of copepods over the shelf, either by favouring cross-shelf processes, drifting organisms northwards from southern areas or advecting them from nearby fjords when at its strongest levels.

Intensive eddy activity in the Lofoten basin has been detected previously by Gaardsted et al (2010), who proved their contribution, along with a patchy horizontal copepod distribution, to strong mesoscale variability in abundance. Eddies can extend to depths greater than 500 m (Smith, 1988), but the most pronounced contrasts in temperature are mostly found in the upper 25−50 m, matching with the average depth limit of the observed patches. Swirls and tendrils extending out from the shelf-break into the deep ocean were observed in the satellite images *(Figure 19)*, possibly reflecting water flows associated with eddies and bathymetric features on the continental slope. The location of these possible eddies matches with the outer edge of transect S3, meaning they could be responsible for the lower temperatures found in the first 500 m of the temperature profile of station 9 compared to the other off-shelf stations. This could be associated with horizontal mixing of the NAC and NCC, and with the notable vertical mixing of the water column reflected by the SSL and the net data from station 9. Such phenomenon, frequently found along the continental slope and in the Lofoten Basin, has already been suggested to provide favourable retention, and thus aggregation areas for the overwintering population of *C. finmarchicus* (Halvorsen et al., 2003). Increased plankton concentrations within eddies compared to the outside region have been detected by Huntley et al (1995) and Pinca and Huntley (2000), proving eddies are centres of plankton concentration. However, a temperature model of the area would be a more accurate way of confirming the presence of these features, and thus their effect on the distribution of organisms in the study area.

On another hand, not only the great hydrographic features affect the distribution of *C. finmarchicus*, but also local driven forces such as coastal winds and waves can affect transport of coastal plankton, redistributing plankton patches. Bloom centres may be typical of the region, attracting grazer species in spring, and can be explained by local hydrographic conditions. Aggregation can also occur as an effect of small scale and not only large scale currents. Possible up and down motion within a water mass could accumulate organisms by convergence. This would leave us with two possible scenarios; one active, where organisms swim actively against the vertical motion created by convergence and thus aggregate at surface, and one passive where they aggregate at surface as an effect of their buoyancy and drift with the prevailing currents in the area. Weidberg et al (2014) suggested upward-swimming or buoyant organisms may aggregate due to convergence in surface flow and the associated subduction, provided that their upward velocity is faster than the downward movement of water. Although considered a weak horizontal swimmer, *C. finmarchicus* can swim effectively in the vertical axis using the cruise and sink behaviour (Mauchline, 1998). With a swimming speed of 1.23 mm/s (Hardy and Brainbridge, 1954), this species could easily overcome downward water movement to remain in surface waters. Observations of upward swimming against downward frontal flows in mero and zooplankton have been reported by Genin et al (2005), who showed that complete depth retention by zooplankton could develop dense aggregations. Suggested adaptive benefits of depth retention could be remaining within layers of high food concentration and increasing the chances of finding a mate within the aggregations generated through depth-keeping in vertical flows (Genin et al., 2005). Unfortunately, lack of acoustic data for the upper 12 m of the water column disables us from observing possible small scale surface discontinuities as an effect of convergence in the hereby described extensive patch.

4.5 Biological drivers

Biological drivers of plankton aggregations have often been overlooked, since most studies tend to focus on physical processes (Folt and Burns, 1999). As proved by other studies (e.g., Folt and Burns, 1999), considering only physical processes would result in an incomplete explanation of many spatial patterns. For instance, Basedow et al. (2010) concluded the depth distribution of older development stages (CV and adults) of *C. finmarchicus* during the productive season in the Subarctic was best predicted by biotic factors such as depth of the fluorescence maximum and population density, instead of abiotic factors such as depth of the pycnocline, which was of secondary importance.

Brierly and Cox (2016) defined obtaining enough oxygen to satisfy metabolic demands and predation avoidance as the two most basic short-term objectives of any organism, meaning they could both be pertinent in explaining the aggregating behaviour of zooplankton. The effect of dissolved oxygen on the distribution and diversity of zooplankton is considered an indirect effect reflected through their oxygen demand as a result of temperature or other environmental stress (Roman et al., 1993). Oxygen consumption by various zooplankton species was examined by Clarke and Peck (1991), who confirmed its direct relation to temperature. Thus, one could assume that copepods aggregating in warm waters to increase their metabolism and growth will require higher oxygen concentrations. However, according to Marshall et al (1935), *Calanus* starts to be affected when oxygen concentrations are below 3 ml O_2/l, but has been observed at concentrations below 1 ml O_2/l. These values are very far from the 9.55 ml O_2/l mean oxygen concentration found here, implying that despite oxygen consumption usually being higher during spring due to the high feeding rates and active reproduction taking place, lack of oxygen within the aggregation was not a limiting factor.

In contrast, reduced predation risk at high densities could be an important driver for zooplankton aggregating in response to predator threat. The larger the aggregation size, the smaller the probability of being eaten (Brierly and Cox, 2016). Thus, despite predation risk being highest in the photic layer due to better visibility, organisms could defy persistence at surface to graze the high phytoplankton concentrations by forming large aggregations. High abundances of zooplankton set an attractive scenario for predator species. By subtracting the 38 from the 120 kHz frequency we can observe a stronger backscatter at 38 kHz within the zooplankton patch, which suggests predator presence. According to Huse et al (2012), the *C. finmarchicus* stock size is negatively correlated to total pelagic fish stock size in the Norwegian Sea, enhancing predator influence on patch formation in the form of top down controls at a large scale. This suggests that seasonally migrating fish species strongly influence the timing of spawning and descent, and hence the formation of *C. finmarchicus* aggregations.

Kaartvedt (2000) stated that Norwegian spring spawning herring *(Clupea harengus)* was the most relevant predator in this context, as they represent the largest fish stock and are the first to initiate feeding migrations. This species accounts for the consumption of 20 to 100% of the annual *C. finmarchicus* production (Dommasnes et al., 2004). They spawn on the Norwegian shelf in February/March, and are present in the eastern Norwegian Sea by mid-April (Misund et al., 1998), before the spring bloom. Østvedt (1965) revealed high abundances of young herring in April, when the overwintering *Calanus* population dominates, and in June, when the new generation has developed into late copepodite stages. This means that the distribution of herring is confined to areas where late copepodite stages (IV and older), either from the overwintering or the new generation, of *C. finmarchicus* predominate. Feeding on stage IV and older stages of *C. finmarchicus* together with feeding on female rather than male copepods may be energetically beneficial for the herring due to their larger body size. Although intermediate stages of *C. finmarchicus* prevailed in our samples, high abundances of CIV and older stages were also present, especially below 30 m, which agrees with the depth at which the high 38 kHz signal was detected. Since herring do not have a swim bladder, individual fish will have a low backscatter at this frequency. This means our observations infer they must be schooling, a common behaviour associated to this species (Gallego and Heath, 1994). Thus, the strong backscatter could be associated to the presence of herring schools feeding on old *C. finmarchicus* stages within the aggregation.

Furthermore, the larvae of many fish species such as Atlantic Cod *(Gadus morhua)* also feed on copepod eggs and nauplii, and copepodite stages are an important food source for the juvenile fish in shelf and shallow sea nursery areas (Runge and de Lafontaine, 1996; Heath and Lough, 2007). Bjørke and Sundby (1984) concluded that the distribution of cod larvae in northern Norway is confined to coastal water masses which flow over the continental shelf. Sixty-four to eighty-four of cod larvae were found between 0-13 m, together with highest abundances found at salinities ranging from 34.3 to 34.6 psu. Similar salinities were found in surface waters above the continental shelf during this study, and the population of cod larvae seemed to be restricted to this water mass and to the vertical distribution of copepod nauplii, which concentrated at the surface. Since the survey was conducted in late April, most larvae were still in a low developmental stage, where they mainly prey on copepod nauplii at first-feeding, switching to older copepodite stages as they grow (Hamre, 2006). A positive correlation between the abundances of cod larvae and copepod nauplii was found in the study area *(Figure 17)*. Although this was only marginally significant, we must take into account the limitations imposed by the small sample size, since marginal effects tend to be statistically significant when the sample size is large enough (Figuereido Filho et al., 2019). This suggests that cod larvae developing on the Lofoten-Vesterålen shelf grow in a favourable environment with high prey abundances for an extended period of time. Since the highest abundances of cod larvae were found at shelf stations, agreeing with the distribution of nauplii, we conclude that the high copepod concentrations found at the surface above the shelf had already attracted cod larvae from their spawning grounds.

These results are not far from expectations, since cod spawns in March and April in coastal water masses close to the coast and mainly in the Lofoten area (Ellertsen et al., 1989). Thus, they do not require long periods of time to be advected by the NCC from their nearby spawning grounds to the study area, where they were already found by late April/ early May. An example of this migration was tracked by Ellertsen et al (1984), where organisms drifted to shelf areas off the west coast of Lofoten from their spawning grounds in the Austnesfjord, Henningsvaer-

Hølla area, inside Vestfjorden. We detected the highest number of cod larvae at station 7, the closest to the mouth of Vestfjorden and hence closest to these spawning grounds. Vlymen (1977) hypothesized that survival of fish larvae in the open sea depends on the existence of forage patchiness. Thus, the fate of the Lofoten cod population, target of one the world's largest seasonal fisheries, could be tightly tied to the occurrence of zooplankton patches in the area.

This study found a negative correlation between chaetognath and total zooplankton abundance. Recognized as one of the most important groups of pelagic predators, this phylum principally predates on copepods, with the consequent effect in the copepod population dynamics (Reeve, 1970). Practically all prey items identified by Saito and Kiørboe (2001) in the guts of *S. elegans*, species present in our net samples, were copepods, 99% being copepodite stages. Moreover, gut content of this species performed by Falkenhaug (1991) in the nearby Barents Sea revealed *C. finmarchicus* was one of the main components of this chaethognath's diet. Thus, decreased zooplankton abundance at stations with higher chaethognath concentrations could be related to copepod predation by this phylum, suggesting significant impact on the structuring of the patch.

Wishner et al (1988) proposed that whales could aggregate in areas of increased abundances of zooplankton. However, whale species feeding on *C. finmarchicus*, such as right whales *(Eubalaena glacialis)*, have not been observed in the study area since 1999 (Jacobsen et al., 2006), meaning that predation pressure exerted by whales on the aggregations encountered is probably null. Other potential predators could be gelatinous zooplankton and other fish species such as blue whiting *(Micromesistius poutassou*) and mackerel *(Scomber scombrus)* (Kaartvedt, 2000), but these species arrive later than herring on the Norwegian Sea feeding grounds, mostly around June. The G0 generation of *C.finmarchicus* would largely have disappeared by that time, meaning these predators mainly feed on G1 animals. Still, relationships between the increase in the recruitment of blue whiting and the reduction in the *C. finmarchicus* stock have been found by Skjoldal (2004).

However, if predation was the only force driving the shape of the aggregation, a shape providing the smallest surface area and an interior position within such structure would be ideal to ensure an individual's survival (Brierly and Cox, 2016). In this sense, a sphere would be a practical shape. Nonetheless, the patch detected by this study presented a completely different layout, consisting of a layer of organisms at surface which decreases in density with depth. Moreover, Skjoldal et al (2003) described *C. finmarchicus*' body size optimum for life in this area, since it is big enough to enable overwintering in a non-feeding mode and at the same time small enough to avoid excessive predation mortality by visual predators feeding in the euphotic zone, where herbivores necessarily feed on phytoplankton. This means other relevant driving forces shaping the patch must exist, so that trade-off by individuals between such driving forces and predator avoidance could determine its shape.

In this sense, judging by the distribution of organisms in the water column, PP at surface seems to be the main biological driver of patchiness through trophic interactions leading to a zooplankton population increase. Positive correlations between zooplankton and phytoplankton abundances have been previously observed at different horizontal and vertical scales (e.g., Marshall and Orr, 1955). Mullin and Brooks (1976) classified phytoplankton aggregations as necessary for successful feeding by *Calanus*, since average concentrations in the water column are often too low. Moreover, Basedow et al (2010) found vertical position was selected by copepods primarily in response to phytoplankton availability during the productive season in the Subarctic. This could be attributed to the high dependency of the reproductive and developmental efficiency of zooplankton populations on the "match" between primary and secondary production. Thus, remaining in the productive upper layer during the bloom could maximize fitness of *C. finmarchicus*.

Maximum chlorophyll concentrations regularly correspond to maximum phytoplankton production, both occurring near the surface. Our water samples revealed the highest chlorophyll values within the top 10-20 m, rapidly decreasing below these depths. This means most of the PP is occurring at the top 12 % of the water column, suggesting phytoplankton surface layering as production hotspots. A similar surface aggregation of *Calanus* species was found by Marshall and Orr (1955) during summer months, where high levels of chlorophyll are registered at surface. Wishner et al (1988) found the highest abundances of zooplankton in surface aggregations within the upper 20 m, with relatively high concentrations extending down to 30 m.

Skjoldal (2004) found a clear temporal trend in the development of phytoplankton biomass from coastal, shelf areas to deeper oceanic areas. Evidence of the bloom start was found in the NCC as soon as March, with full bloom development occurring in April, while oceanic areas did not present high phytoplankton biomass until May. This could have attracted high abundances of *C. finmarchicus* adult females to spawn in shelf areas as early as chlorophyll *a* concentrations were sufficient to fuel egg maturation and growth. The presence of diverse developmental stages in the net samples collected suggests active growth, and together with the annual occurrence of this phenomenon emphasizes a relation to productivity. Thus, high numbers of grazers detected by our study over the shelf compared to less densely populated off-shelf areas could simply accumulate due to the earlier start of the bloom in the NCC. This would provide an early source of food to boost the development of the G1 generation before predators are attracted to the area later in the season.

Compared to typical spring bloom concentrations, we found generally low chlorophyll *a* values at most stations. These results are in line with those described by Skjodal (2004), who seldom found chlorophyll *a* concentrations higher than 3 mg/m^3 during the spring bloom. Highest zooplankton abundances have been found in the top 30 m of the water column, matching with the highest chlorophyll *a* values and thus confirming their affinity to phytoplankton rich layers and the importance of the spring bloom for reproduction and growth of *C. finmarchicus*. However, the close match between the bloom and the development of the zooplankton community proposes grazing as a relevant factor in controlling the size of the bloom, especially during the developmental period, when grazing pressure is strongest. The BEST analysis revealed nitrate+nitrite instead of chlorophyll *a* as one of the main factors explaining the zooplankton distribution. This suggests the nutrient rich waters from the start of the bloom drive high levels of PP, which are subject to strong grazing pressure by the high abundances of zooplankton, triggering the low chlorophyll *a* values found in our samples. Therefore, phytoplankton biomass during the spring bloom might not reach the potential concentrations we could expect in a system without grazers, meaning top-down control via grazing pressure by *C. finmarchicus* plays a significant role in regulating the bloom's size. This suggests nitrate+nitrite as a better predictor of the zooplankton aggregation than chlorophyll *a* in similar scenarios involving top-down control.

Similar results were found by Bathmann et al (1990), where the strong grazing pressure exerted by *C. finmarchicus* during its developmental period on the mixed phytoplankton stock and its selective grazing on diatoms, main component of the phytoplankton spring bloom, prevented the blooming of this phytoplankton group. This could explain the stronger sedimentation of the spring phytoplankton bloom out of the euphotic zone in the absence of overwintering copepods migrating to the upper layers experimented by Slagstad and Wassmann (1996).

Benoit-Bird et al. (2010), confirmed the importance of phytoplankton layer formation in zooplankton distribution by tracking both phyto and zooplankton signals using acoustics. They concluded that when minimum 18% of the phytoplankton biomass aggregated in layers, their association was highest. This suggests grazing rates within phytoplankton layers could be significantly higher than outside such aggregations. Meyer-Harms et al (1999) observed high clearance rates by *C. finmarchicus* adult females ranging from 22 to 100 ml copepod^{-1} day^{-1} in the Norwegian Sea at the same time of the year. These results are in agreement with those obtained by Møller et al (2012), who detected clearance rates of 90 ml copepod^{-1} day^{-1} by *C. finmarchicus* adult females and CIVs in surface waters at 6.3°C, a very similar temperature to those registered in our study area. Although clearance rates for *C. finmarchicus* peaked at 14°C, we observed higher filtration rates of this species at low temperatures compared to other calanoids. Moreover, by multiplying the abundance of *C. finmarchicus* sampled in the upper 5 m by the filtration rates obtained by Meyer-Harms et al (2002), the following filtration rates in ml day^{-1} will result for each developmental stage: *CI: 43260, CII: 134285.5, CIII: 569026.2, CIV: 288019.3, CV: 267326.2, AF: 136704.1*. Such clearance rates suppose a high grazing pressure on the available PP, meaning although the nutrient analysis confirmed high amounts of PP could be supported, they are rapidly cleared by the high grazing pressure exerted by the rich abundance of *C. finmarchicus* at surface. Thus, we can propose nutrient rich waters which act as a source of surface phytoplankton layers, as an important driver for the accumulation of zooplankton, leading to further patch formation in the study area.

5 Conclusion

This study presents a comprehensive view of zooplankton patchiness in the Lofoten-Vesterålen region. Here we report a large scale aggregation of *C. finmarchicus* observed over the whole continental shelf, closely tied to the distribution of the NCC and its cold, fresh and nutrient-rich waters. Stable, stratified conditions provided by this current triggered an early start of the bloom, attracting high abundances of this grazer species to benefit from PP occurring at surface. Dominance of intermediate copepodite stages suggested rapid development through intensive grazing, which could further enable an early descent into overwintering layers, anticipating the arrival of its main predators. Thus, through thorough examination of hydrographic, acoustic and ground data, we can conclude biological structures can be correlated to the hydrography over large spatial scales and ecological interactions may drive habitat selection by planktonic organisms even in highly fluctuating oceanic environments. Thus, trade-off between physical and biological drivers will determine patch formation, morphology and composition.

Further research is required to uncover unknown aspects of zooplankton patchiness, such as persistence and frequency of occurrence, details of its main components and their origin, and its ecological consequences. Although increased resolution achieved through the introduction of acoustic and optical methods has improved our understanding of such features, progress in addressing this phenomenon in further detail will be hindered when mapping zooplankton abundance and distributions from ships, due to the disturbance of the environment through the physical invasion of the water column and the severe spatio-temporal limitations. Hence, development of autonomous platforms providing continuous data in time and space together with remote detection of such aggregations will be crucial for increasing our understanding of *C. finmarchicus* aggregative behaviour and will improve sustainable management of this harvested key species.

6 Acknowledgments

This research was supported by the Sea Patches project and the University of Tromsø. I thank this institution for providing the fully equipped *R/V Helmer Hanssen* and laboratories together with the pertinent facilities and funding. In addition, I thank the ship's crew and participants for running a fabulous expedition and their help in assisting with the sampling processes. Lastly, I would also like to show my special gratitude to Dr. Sünnje Basedow for giving me the opportunity of taking part in the project and, together with Dr. Maxime Geoffroy and Dr. Nicolás Weidberg López, for providing insight and expertise that greatly assisted the research.

7 References

Aarflot, J.M., Skjoldal, H.R., Dalpadado, P., Skern-Mauritzen, M., 2017. Contribution of Calanus species to the mesozooplankton biomass in the Barents Sea. ICES Journal of Marine Science 75 (7): 2342–2354.

Aksnes, D.L., Magnesen, T., 1988. A population dynamics approach to the estimation of production of four calanoid copepods in Lindåspollene, western Norway. Marine Ecology Progress Series 45: 57–68.

Ådlandsvik, B., and Sundby, S., 1994. Modelling the transport of cod larvae from the Lofoten area. ICES Marine Science Symposia 198: 379–392.

Ambler, J.W., 2002. Zooplankton swarms: characteristics, proximal cues and proposed advantages. Hydrobiologia 480: 155−164.

Backhaus, J.O., Harms, I.H., Krause, M., Heath, M.R., 1994. An hypothesis concerning the space-time succession of Calanus finmarchicus in the northern North Sea. ICES Journal of Marine Science 51: 169–180.

Bagoeien, E., Melle, W., Kaartvedt, S., 2012. Seasonal development of mixed layer depths, nutrients, chlorophyll and Calanus finmarchicus in the Norwegian Sea – a basin-scale habitat comparison. Progress in Oceanography 103: 58–79.

Basedow, S.L., Tande, K.S., 2006. Cannibalism by female Calanus finmarchicus on naupliar stages. Marine Ecology Progress Series 327: 247–255.

Basedow, S.L., Tande, K., Stige, L., 2010. Habitat selection by a marine copepod during the productive season in the Subarctic. Marine Ecology Progress Series 416: 165–178.

Basedow, S.L., McKee, D., Lefering, I., Gislason, A., Daase, M., Trudnowska, E., Egeland, E.S., Choquet, M., Falk-Petersen, S., 2019. Remote sensing of zooplankton swarms. Scientific Reports: 9.

Bathmann, U., Noji, T., von Bodungen, B., 1990. Copepod grazing potential in late winter in the Norwegian Sea - A factor in the control of spring phytoplankton growth? Marine Ecology Progress Series 60: 225–233.

Behrenfeld, M.J., 2010. Abandoning Sverdrup’s Critical Depth Hypothesis on phytoplankton blooms. Ecology 91: 977–989.

Benoit-Bird, K.J., Moline, M.A., Waluk, C.M., Robbins, I.C., 2010. Integrated measurements of acoustical and optical thin layers I: Vertical scales of association. Continental Shelf Research 30: 17−28.

Bjørke, H., Sundby, S., 1984. Distribution and abundance of post-larval Northeast arctic cod and haddock. In Proceedings of the Soviet-Norwegian Symposium on Reproduction and Recruitment of Arctic Cod: 72−92.

Blindheim, J., 1990. Arctic intermediate water in the Norwegian Sea. Deep-Sea Research Part I 37 (9): 1475–1489.

Blindheim, J., 2004. Oceanography and climate. The Norwegian Sea Ecosystem: 65–96.

Bollens, S.M., Osgood, K., Frost, B.W., Watts, S.D., 1993. Vertical distributions and susceptibilities to vertebrate predation of the marine copepods *Metridia lucens* and *Calanus pacificus*. Limnology and Oceanography 38 (8): 1827–1837.

Brentnall, S.J., Richards, K.J., Murphy, E., Brindley, J., 2003. Plankton patchiness and its effect on larger-scale productivity. Journal of Plankton Research 25 (2): 121–140.

Brinton, E., 1967. Vertical migration and avoidance capability of euphausiids in the California Current. Bulletin of the Scripps Institution of Oceanography 12: 451–483.

Brock, V.E., Riffenburgh, R.H., 1960. Fish schooling: a possible factor in reducing predation. ICES Journal of Marine Science 25: 307–317.

Broms, C., Melle, W., Kaartvedt, S., 2009. Oceanic distribution and life cycle of Calanus species in the Norwegian Sea and adjacent waters. Deep-Sea Research Part II 56: 1910–1921.

Chu, D., Wiebe, P.H., Copley, N.J., Lawson, G.L., Puvanendran, V., 2003. Material properties of North Atlantic cod eggs and early-stage larvae and their influence on acoustic scattering. ICES Journal of Marine Science 60: 508–515.

Clarke, A., Peck, L.S., 1991. The physiology of polar marine zooplankton. Polar Research 10 (2): 355–369.

Conover, R.J., 1988. Comparative life histories of the genera *Calanus* and *Neocalanus* in high latitudes of the northern hemisphere. Hydrobiologia 167 (168): 27–142.

Cottier, F.R., Tarling, G.A., Wold, A., Falk Petersen, S., 2006. Unsynchro-nized and synchronized vertical migration of zooplankton in a high arctic fjord. Limnology and Oceanography 51: 2586–2599.

Coyle, K.O., Pinchuk, A.I., 2005. Seasonal cross-shelf distribution of major zooplankton taxa on the northern Gulf of Alaska shelf relative to water mass properties, species depth preferences and vertical migration behaviour. Deep-Sea Research Part II 52: 217–245.

Cushing, D.H., Tungate, D.S., 1963. Studies on a *Calanus* patch. The identification of a *Calanus* patch. Journal of the Marine Biological Association of the United Kingdom 43: 327–337.

Daase, M., Eiane, K., Aksnes, D.L., Vogedes, D., 2008. Vertical distribution of *Calanus* spp. and *Metridia longa* at four Arctic locations. Marine Biology Research 4 (3): 193–207.

Dalpadado, P., Ellertsen, B., Melle, W., Dommasnes, A., 1998b. Food and feeding conditions and prey selectivity of herring *(Clupea harengus)* through its feeding migrations from coastal areas of Norway to the Atlantic and Arctic watermasses of the Nordic Seas. ICES Journal of Marine Science 57 (4): 843–857.

Debby, L., Jackson, G.A., Angel, M.V., Lampitt, R.S., Burd, A.B., 2004. Effect of net avoidance on estimates of diel vertical migration. Limnology and Oceanography 46: 2297–2303.

Dommasnes, A., Melle, W., Dalpadado, P., Ellertsen, B., 2004. Herring as a major consumer in the Norwegian Sea. ICES Journal of Marine Science 61: 739–751.

Edvardsen, A., Petersen, J.M., Slagstad, D., Semenova, T., Timonin, A., 2006. Distribution of overwintering Calanus in the North Norwegian Sea. Ocean Science 2: 87–96.

Eilertsen, B., Fossum, P., Solemdal, P., Sundby, S., Tilseth, S., 1984. A case study on the distribution of cod larvae and availability of prey organisms in relation to physical processes in Lofoten. In the propagation of cod *(Gadus morhua)*: 453–478.

Eilertsen, H.C., Taasen, J.P., 1981. Diel variatons in some important phytoplankton parameters during a 24 hours sampling period in Balsfjorden, Tromsø and Skjomenfjorden, Nordland, North Norway. Kieler Meeresforscherung 5: 68-81.

Elith, J., Leathwick, J.R., 2009. Species distribution models: ecological explanation and prediction across space and time. Annual Review of Ecology, Evolution and Systematics 40: 677–697.

Espinasse, B., Basedow, S., Hattermann, T., Nøst, O.A., Albretsen, J., Skardhamar, J., Eiane, K., 2016. Mechanisms regulating inter-annual variability in zooplankton advection over the Lofoten shelf, implications for cod larvae survival. Fisheries Oceanography 26: 299–315.

Falkenhaug, T., 1991. Prey composition and feeding rate of *Sagitta elegans* (chaetognatha) in the Barents Sea in early summer. Polar Research 10 (2): 487–506.

Falkenhaug, T., Tande, K.S., Timonin, A., 1997. Spatiotemporal patterns in the copepod community in Malangen, northern Norway. Journal of Plankton Research 19: 449–468.

Figuereido Filho, D.B., Paranhos, R., C. da Rocha, E., Batista, M., da Silva Jr., J.A., Wanderley M.L., Santos, D., Guiro Marinoet, J., 2013. When is statistical significance not significant? Brazilian Political Science Review 7: 31–55.

First update of the Integrated Management Plan for the Marine Environment of the Barents Sea−Lofoten Area, 2011. Norwegian Ministry of the Environment 10. Available at: www.miljodirektoratet.no

Fleminger, A., Clutter, R.I., 1965. Avoidance of towed nets by zooplankton. Limnology and Oceanography 10: 96–104.

Franks, P.J.S., 2005. Plankton patchiness, turbulent transport and spatial spectra. Marine Ecology Progress Series 294: 295−309.

Frontier, D., Lepretre, A., Davoult, D., Luczak, C., 2004. Ecosystemes—Structure, Fonctionnement, Evolution. Dunod.

Folt, C.L., Burns, C.W, 1999. Biological drivers of zooplankton patchiness. Trends in Ecology and Evolution 14: 300–305.

Gaard, E., Hansen, B., 2000. Variations in the advection of *Calanus finmarchicus* onto the Faroe Shelf. ICES Journal of Marine Science 57: 1612–1618.

Gaardsted, F., Zhou, M., Pavlov, V., Morozov, A., Tande, K.S., 2010. Mesoscale distribution and advection of overwintering *Calanus finmarchicus* off the shelf of northern Norway. Deep-Sea Research Part I 57: 1465–1473.

Gallager, S.M., Davis, C.S., Epstein, A.W., Solow, A., Beardsley, R.C., 1996. High-resolution observations of plankton spatial distributions correlated with hydrography in the Great South Channel, Georges Bank. Deep-Sea Research Part II 43 (7-8): 1627–1663.

Gallego, A., Heath, M., 1994. The development of schooling behaviour in Atlantic herring *(Clupea harengus)*. Journal of Fish Biology 45: 569–588.

Gascard, J.C., Raisbeck, G., Sequeira, S., Yiou, F., Mork, K.A., 2004. The Norwegian Atlantic Current in the Lofoten basin inferred from hydrological and tracer data (129I) and its interaction with the Norwegian Coastal Current. Geophysics Research Letter 31.

Genin, A., Jaffe, S.J., Reef, R., Richter, C., Franks, P.J.S., 2005. Swimming against the flow: a mechanism of zooplankton aggregation. Science 308: 860−862.

Geoffroy, M., Cottier, F.R., Berge, J. and Inall, M.E., 2016. AUV-based acoustic observations of the distribution and patchiness of pelagic scattering layers during midnight sun. ICES Journal of Marine Science 74: 2342–2353.

Gislason, A., Astthorsson, O.S., Petursdottir, H., Gudfinnsson, H. and Bodvarsdottir, A.R., 2000. Life cycle of *Calanus finmarchicus* south of Iceland in relation to hydrography and chlorophyll *a*. ICES Journal Marine Science 57: 1619–1627.

Godø, O.R., Samuelsen, A., Macaulay, G.J., Patel, R., Hjøllo, S.S., Horne, J., Kaartvedt, S., Johannessen, J.A., 2012. Mesoscale eddies are oases for higher trophic marine life. PLOS ONE 7.

Gómez-Gutiérrez, J., Martínez-Gómez, S., Robinson, C.J., 2007. Influence of thermo-haline fronts forced by tides on near-surface zooplankton aggregation and community structure in Bahía Magdalena, Mexico. Marine Ecology Progress Series 346: 109–125.

Guisan, A., Zimmermann, N.E., 2000. Predictive habitat distribution models in ecology. Ecological Modelling 135: 147–186.

Halvorsen, E., Tande, K.S., 1999. Physical and biological factors influencing the seasonal variation in distribution of zooplankton across the shelf at Nordvestbanken, northern Norway, 1994. Sarsia 84: 279–292.

Halvorsen, E., Tande, K.S., Edvardsen, A., Slagstad, D., Pedersen, O.P., 2003. Habitat selection of overwintering *Calanus finmarchicus* in the NE Norwegian Sea and shelf waters off Northern Norway in 2000–02. Fisheries Oceanography 12: 339–351.

Hamre, K., 2006. Nutrition in cod *(Gadus morhua)* larvae and juveniles. ICES Journal of Marine Science 63 (2): 267–274.

Hardy, A.C., Brainbridge, R., 1954. Experimental observations on the vertical migrations of planktonic animals. Journal of the Marine Biological Association of the United Kingdom 33: 409–448.

Haury, L.R., McGowan, J.A., Wiebe, P.H., 1978. Patterns and processes in the time-space scales of plankton distributions. Spatial pattern in plankton communities (Steele, J.H., ed.): 277–326.

Haury, L.R., Wiebe, P.H., 1982. Fine-scale multi-species aggregations of oceanic zooplankton. Deep-Sea Research Part I 29: 915–921.

Heath, M.R., Astthorsson, O.S., Dunn, J., Ellertsen, B., Gaard, E., Gislason, A., Gurney, W.S.C., Hind, A.T., Irigoien, X., Melle, W., Niehoff, B., Olsen, K., Skreslet, S., Tande, K.S., 2000a. Comparative analysis of *Calanus finmarchicus* demography at locations around the Northeast Atlantic. ICES Journal of Marine Science 57: 1562–1580.

Heath, M., Lough, R., 2007. A synthesis of large-scale patterns in the planktonic prey of larval and juvenile cod *(Gadus morhua).* Fisheries Oceanography 16 (2): 169–185.

Hirche, H.J., 1996a. Diapause in the marine copepod, *Calanus finmarchicus* – a review. Ophelia 44: 129–143.

Hirzel, A.H., Hausser, J., Chessel, D., Perrin, N., 2002. Ecological-niche factor analysis: how to compute habitat-suitability maps without absence data? Ecology 83: 2027–2036.

Horne, J.K., 2000. Acoustic approaches to remote species identification: a review. Fisheries Oceanography 9: 356–371.

Huntley, M.E., Zhou, M., Nordhausen, W., 1995. Mesoscale distribution of zooplankton in the California Current in late spring, observed by optical plankton counter. Journal of Marine Research 53: 647–674.

Huse, G., Holst, J.C., Utne, K., Nottestad, L., Melle, W., Slotte, A., Ottersen, G., Fenchel, T., Uiblein, F., 2012. Effects of interactions between fish populations on ecosystem dynamics in the Norwegian Sea – results of the INFERNO project Preface. Marine Biology Research 8: 415–419.

Jacobsen, K-O., Marx, M., Øien, N., 2006. Two-way trans-Atlantic migration of a North Atlantic right whale *(Eubalaena glacialis)*. Marine Mammal Science 20: 161–166.

Johannesen, E., Ingvaldsen, R.B., Bogstad, B., Dalpadado, P., et al., 2012. Changes in Barents Sea ecosystem state, 1970-2009: Climate fluctuations, human impact, and trophic interactions. ICES Journal of Marine Science 69: 880–889.

Krause, M., Radach, G., 1989. On the relations of vertical distribution, diurnal migration and nutritional state of herbivorous zooplankton in the northern North-Sea during Flex 1976. International Revue ges Hydrobiology 74: 371–417.

Krause, M., Trahms, J., 1982. Vertical distribution of copepods (all developmental stages) and other zooplankton during spring bloom in the Fladen Ground area of the North Sea. Netherlands Journal of Sea Research 16: 217–230.

Kongsberg Maritime AS, 2017. Simrad EK60. Available at: https://www.simrad.com/ek60.

Kosobokova, K.N., Hopcroft, R.R., 2010. Diversity and vertical distribution of mesozooplankton in the Arctic's Canada Basin. Deep-Sea Research Part II 57: 96–110.

Koszalka, I., LaCasce, J.H., Andersson, M., Orvik, K.A., Mauritzen, C., 2011. Surface circulation in the Nordic Seas from clustered drifters. Deep-Sea Research Part I 58: 468–485.

Langøy, H., Nøttestad, L., Skaret, G., Broms, C., Ferno, A., 2012. Overlap in distribution and diets of Atlantic mackerel *(Scomber scombrus)*, Norwegian spring spawning herring *(Clupea harengus)* and blue whiting *(Micromesistius poutassou)* in the Norwegian Sea during late summer. Marine Biology Research 8: 442–460.

Kvile, K.Ø., Dalpadado, P., Orlova, E., Stenseth, N.C., Stige, L.C., 2014. Temperature effects on *Calanus finmarchicus* vary in space, time and between developmental stages. Marine Ecology Progress Series 517: 85–104.

Lamb, J., Peterson, W., 2005. Ecological zonation of zooplankton in the COAST study region off central Oregon in June and August 2001 with consideration of retention mechanisms. Journal of Geophysical Research 110.

Lawson, G.L., Wiebe, P.H., Ashjian, C.J., Stanton, T.K., 2008. Euphausiid distribution along the Western Antarctic Peninsula. Part B: distribution of euphausiid aggregations and biomass, and associations with environmental features. Deep-Sea Research Part II 55: 432–454.

Levin, SA, 1992. The problem of pattern and scale in ecology: the Robert H. MacArthur Award Lecture. Ecology 73: 1943–1967.

Longhurst, A.R., Harrison, W.G., 1989. The biological pump – profiles of plankton production and consumption in the upper ocean. Progress in Oceanography 22: 47–123.

López-Urrutia, A., Harris, R.P., Smith, T., 2004. Predation by calanoid copepods on the appendicularian *Oikopleura dioica*. Limnology and Oceanography 49: 303–307.

Mahavedan, A., D'Asaro, E., Lee, C., Perry, M.J., 2012. Eddy-driven stratification initiates North Atlantic spring phytoplankton blooms. Science 337: 54–58.

Mann, K.H., Lazier, J.R.N., 1996. Dynamics of Marine Ecosystems; Biological Physical Interactions in the Ocean 2. Blackwell Science: 394.

Marshall, S.M., Nicholls, A.G., Orr, A.P., 1935. On the Biology of *Calanus finmarchicus*. Part VI: Oxygen Consumption in Relation to Environmental Conditions. Journal of The Marine Biological Association of The United Kingdom 20.

Marshall, S.M., Orr, A.P., 1972. The Biology of a Marine Copepod *Calanus finmarchicus* Gunnerus. Springer Verlag.

Mauchline, J., 1998. The biology of calanoid copepods. Academic Press.

Melle, W., Ellertsen, B., Skjoldal, H.R., 2004. Zooplankton: the link to higher trophic levels. The Norwegian Sea Ecosystem: 137–202.

Melle, W., Runge, J., Head, E., Plourde, S., Castellani, C., Licandro, P., Pierson, J., Jonasdottir, S., Johnson, C., Broms, C., Debes, H., Falkenhaug, T., Gaard, E., Gislason, A., Heath, M., Niehoff, B., Nielsen, T.G., Pepin, P., Stenevik, E.K., Chust, G., 2014. The North Atlantic Ocean as habitat for *Calanus finmarchicus*: environmental factors and life history traits. Progress in Oceanography 129: 244–284.

Menden-Deuer, S., 2012. Structure-Dependent phytoplankton photosynthesis and production rates: Implications for the formation, maintenance, and decline of plankton patches. Marine Ecology Progress Series 468: 15-30.

Meyer-Harms, B., Irigoien, X., Graeve, M., Head, R.N., Harris, R.P., 2002. Feeding rates and selectivity among nauplii, copepodites and adult females of *Calanus finmarchicus* and *Calanus helgolandicus*. Helgoland Marine Research 55 (3): 169–176.

Meyer-Harms, B., Irigoien, X., Head, R.N., Harris, R.P., 1999. Selective feeding on natural phytoplankton by *Calanus finmarchicus* before, during, and after the 1997 spring bloom in the Norwegian Sea. Limnology and Oceanography 44: 154–65.

Misund, O.A., Vilhjálmsson, H., Jákupsstovu, S.H., et al., 1998. Distribution, migration and abundance of Norwegian spring spawning herring in relation to the temperature and zooplankton biomass in the Norwegian Sea as recorded by coordinated surveys in spring and summer 1996. Sarsia 83: 117–127.

Mitchelson-Jacob, G., Sundby, S., 2001. Eddies of Vestfjorden, Norway. Continental Shelf Research 21: 1901–1918.

Mullin, M.M., Brooks, E.R., 1976. Some consequences of distributional heterogeneity of phytoplankton and zooplankton. Limnology and Oceanography 21: 784–796.

Møller, E.F., Maar, M., Jónasdóttir, S.H., Nielsen, T.G., Tönnesson, K., 2012. The effect of changes in temperature and food on the development of *Calanus finmarchicus* and *Calanus helgolandicus* populations. Limnology and Oceanography 57 (1): 211–220.

Nordby, E., Tande, K.S., Svendsen, H., Slagstad, D., 1999. Oceanography and fluorescence at the shelf break off the north Norwegian coast during the main productive period in 1994. Sarsia 84: 175–189.

Ohman, M.D., Hirche, H.J., 2001. Density-dependent mortality in an oceanic copepod population. Nature 412: 638–641.

Ohman, M.D., Runge, J.A., Durbin, E.G., Field, D.B., Niehoff, B., 2002. On birth and death in the sea. Hydrobiologia 480: 55–68.

Ottersen, G., Bogstad, B., Yaragina, N.A., Stige, L.C., Vikebø, F.B. and Dalpadado, P., 2014. A review of early life history dynamics of Barents Sea cod *(Gadus morhua)*. ICES Journal of Marine Science 71: 2064–2087.

Pedersen, O-P., Tande, K.S., Slagstad, D., 2001. A model study of demography and spatial distribution of *Calanus finmarchicus* at the Norwegian coast. Deep Sea Research Part II 48: 567–587.

Pedersen, O-P., Tande, K.S., Timonin, A., Semenova, T., 2000. A possible connection between hydrography and the distribution of *Calanus finmarchicus* on the Norwegian midshelf in 1997. ICES Journal of Marine Science 57: 1645–1655.

Pinca, S., Huntley, M.E., 2000. Spatial organization of particle size composition in an eddy-jet system off California. Deep-Sea Research Part I 47: 973–996.

Planque, B., Batten, S., 2000. *Calanus finmarchicus* in the North Atlantic: the year of *Calanus* in the context of interdecadal change. ICES Journal of Marine Science 57: 1528–1535.

Reeve, M. R., 1970. The biology of chaetognaths I. Quantitative aspects of growth and egg production in *Sagitta hispida*. Marine Food Chains: 168–189.

Richter, K.E., 1985b. Acoustic determination of small-scale distributions of individual zooplankters and zooplankton aggregations. Deep-Sea Research Part I 32: 163–182.

Rey, F., 2004. Phytoplankton: the grass of the sea. The Norwegian Sea Ecosystem (Skjoldal, H., ed.): 97–136.

Rey-Rassat, C., Irigoien, X., Harris, R., Carlotti, F., 2002. Energetic cost of gonad development in *Calanus finmarchicus* and *Calanus helgolandicus*. Marine Ecology Progress Series 238: 301–306.

Roman, M., Gauzens, A., Rhinehart, W.K., White, J., 1993. Effects of low oxygen waters on Chesapeake Bay zooplankton. Limnology and Oceanography 38: 1603–1614.

Runge, J.A., de Lafontaine, Y., 1996. Characterization of a pelagic food web in the northern Gulf of St. Lawrence: the larval redfish-Calanus-microplankton interaction. Fisheries Oceanography 5: 21–37.

Runge, J.A., Plourde, S., Joly, P., Niehoff, B., Durbin, E., 2006. Characteristics of egg production of the planktonic copepod, *Calanus finmarchicus*, on Georges Bank: 1994–1999. Deep-Sea Research Part II 53: 2618–2631.

Sakshaug, E., Bjørge, A., Gulliksen, B., Loeng, H., Mehlum, F., 1994. Structure, biomass distribution, and energetics of the pelagic ecosystem in the Barents Sea: a synopsis. Polar Biology 14: 405–411.

Sakshaug, E., Tangen, K., Slagstad, D., 2000. Marine primary production and the effects of wind. The Changing Ocean Carbon Cycle. Cambridge University Press: 19–36.

Saito, H., Kiørboe, T., 2001. Feeding rates in the chaetognath *Sagitta elegans*: effects of prey size, prey swimming behaviour and small-scale turbulence. Journal of Plankton Research 23 (12): 1385–1398.

Saumweber, W.J., Durbin, E.G., 2006. Estimating potential diapause duration in *Calanus finmarchicus*. Deep-Sea Research Part II 53: 2597–2617.

Simmonds, E.J., MacLennan, D.N., 2005. Fisheries Acoustics: Theory and Practice, 2nd edition. Blackwell Science: 437.

Skjoldal, H., 2004. The Norwegian Sea ecosystem. Tapir Academic Press: 119–172.

Skjoldal, H.R., Noji, T., Giske, J., Fossa, J.H., Blindheim, J., Sundby, S., 1993. Mare Cognitum. Science plan for research on marine ecology of the Nordic Seas (Greenland, Norwegian, Iceland Seas): 1993–2000.

Skreslet, S., 1997. A conceptual model of the trophodynamical response to river discharge in a large marine ecosystem. Journal of Marine Systems 12: 187–198.

Slagstad, D.L., Tande, K.S., 2007. Structure and resilience of overwintering habitats of Calanus finmarchicus in the Eastern Norwegian Sea. Deep-Sea Research Part II 54: 2702–2715.

Slagstad, D.L., Wassmann, P., 1996. Climatic change and carbon flux in the Barents Sea: 3-D simulations of ice distribution, primary production and vertical export of particulate organic carbon. Memoirs of National Institute of Polar Research 51 (Special Issue): 119–141.

Smith, S.L., 1988. Copepods in Fram Strait in summer: distribution, feeding and metabolism. Journal of Marine Research 46: 145−181.

Sokal, R.R., Rohlf, F.J., 2012. Biometry - The Principles and Practice of Statistics in Biological Research. SERBIULA (sistema Librum 2.0).

SOKI, 2014. HYDRO-BIOS MultiNet - Methods - Confluence, SOKI, Antarctic Climate and Ecosystems Co-operative Research Centre. Available at: http://soki.aq.

Stanton, T.K., Wiebe, P.H., Chu, D., Benfield, C., Scanlon, L.M., Martin, L.L., Eastwood, R., 1994. On acoustic estimates of zooplankton biomass. ICES Journal of Marine Sciences 51.

Stibor, H., Vadstein, O., Lippert, B., Roederer, W., Olsen, Y., 2004. Calanoid copepods and nutrient enrichment determine population dynamics of the appendicularian *Oikopleura dioica*: a mesocosm experiment. Marine Ecology Progress Series 270: 209–215.

Sundby, S., 1984. Influence of bottom topography on the circulation at the continental shelf off northern Norway. Fiskeridirektoratets Skrifter Serie Havundersøkelser 17: 501–519.

Sundby, S., 2000. Recruitment of Atlantic cod stocks in relation to temperature and advection of copepod populations. Sarsia 85 (4): 277–298.

Sætre, R., 1999. Features of the central Norwegian shelf circulation. Continental Shelf Research 19: 1809–1831.

Sverdrup, H.U., 1953. On conditions for the vernal bloom of phytoplankton. ICES Journal of Marine Sciences 18: 287–295.

Tande, K.S., 1988a. Aspects of developmental and mortality rates in *Calanus finmarchicus* related to equiproportional development. Marine Ecology Progress Series 44: 51–58.

Troedsson, C., Bouquet, J.M., Aksnes, D.L., Thompson, E.M., 2002. Resource allocation between somatic growth and reproductive output in the pelagic chordate *Oikopleura dioica* allows opportunistic response to nutritional variation. Marine Ecology Progress Series 243: 83–91.

University of Tromsø (UIT), 2013. FF Helmer Hansen. Available at: https://uit.no/forskning/art?dim=179012&p_document_id=336568.

Weidberg, N., Lobon, C., Lopez, E., Garcia Florez, L., Fernandez Rueda, M., Largier, J.L., Acuna, L., 2014. Effect of nearshore surface slicks on meroplankton distribution: role of larval behaviour. Marine Ecology Progress Series 506: 15–30.

Wiborg, K.F., 1954. Investigations on zooplankton in coastal and offshore waters of western and northwestern Norway. Fiskedirektoratets Skrifter Serie Havundersøkelser 11: 1–246.

Wishner, K., Durbin, E., Durbin, A., Macaulay, M., Winn, H., Kenney, R., 1988. Copepod patches and right whales in the Great South Channel off New England. Bulletin of Marine Science 43: 825–844.

Zhai, L., Gudmundsson, K., Miller, P., Peng, W.J., Gudfinnsson, H., Debes, H., Hatun, H., White, G.N., Walls, R.H., Sathyendranath, S., Platt, T., 2012. Phytoplankton phenology and production around Iceland and Faroes. Continental Shelf Research 37: 15–25.

Østvedt, O.J. 1965. The migration of Norwegian herring to Icelandic waters and the environmental conditions in May-June, 1961-1964. Fiskedirektoratets Skrifter Serie Havundersøkelser 8: 29–47.

8 Appendix

1. Station Overview

Station #	Date	Start Time (UTC)	Latitude	Longitude	CTD Depth	Multinet Depth	Bongo Depth
1	28/04/2017	16:45	68 04.02	09 50.71	1182	-	-
2	28/04/2017	19:00	67 56.05	09 44.05	1147	-	-
3	29/04/2017	8:20	67 38.956	11 36.918	135	-	-
4	29/04/2017	10:56	67 46.858	10 37.811	173	150-100, 100-30, 30-4, 4-2, 2-0	10
5	30/04/2017	6:26	67 54.457	09 50.287	850	820-100, 100-30, 30-5, 5-2, 2-0	15
6	30/04/2017	17:26	67 55.821	10 55.690	173	160-100, 100-30, 30-5, 5-2, 2-0	15
7	30/04/2017	1:05	67 44.765	12 30.783	87	90-50, 50-30, 30-5, 5-2, 2-0	15
8	01/05/2017	15:22	68 34.74	11 50.680	935	1000-650, 650-100, 100-30, 30-5, 5-0	15
9	01/05/2017	23:03	68 44.999	11 29.988	2185	550-100, 100-30, 30-5, 5-2, 2-0	-
10	02/05/2017	15:27	68 24.622	12 10.964	160	160-100, 100-30, 30-5, 5-2, 2-0	15 (Only 200 µm)
11	03/05/2017	3:33	68 28.777	12 25.237	142	130-100, 100-30, 30-5, 5-2, 2-0	15 (Only 200 µm)
12	03/05/2017	8:36	68 37.682	12 06.416	73	465-100, 100-30, 30-5, 5-2, 2-0	15 (Only 200 µm)

2. Acoustic Data Analysis

Species	Density (Ind/m3)	Rel. Abundance	Mean PL (mm)	Length SD	Mean Width (mm)	Mean Weight (g)	Biomass (g/m3)	Rel. Biomass (g/m3)	Mean Ts (dB re 1 m2)	References	MAD (Ind/m3)	MASD (Ind/m3)
Calanus finmarchicus AM	841.5219	0.0127	2.7620	0.1140	1.0154	0.0002	4344460.1980	0.0024	-124.4174	Cottier et al., 2006	51229.3247	648.6808
C. finmarchicus AF	2651.4303	0.0399	3.0135	0.1200	1.1079	0.0003	10132725.7081	0.0056	-117.5093	Cottier et al., 2006		2043.8350
C. finmarchicus CV	6766.9861	0.1018	2.6225	0.0940	0.9642	0.0002	41771519.4048	0.0231	-116.5174	Cottier et al., 2006		5216.2801
C. finmarchicus CIV	14079.1123	0.2118	2.0540	0.0825	0.7551	0.0001	201995872.2623	0.1116	-118.8525	Cottier et al., 2006		10852.7773
C. finmarchicus CIII	29354.2756	0.4417	1.5410	0.0545	0.5665	0.0000	1134245580.1307	0.6266	-122.2909	Cottier et al., 2006		22627.5216
C. hyperboreus AF	5.1380	0.0001	6.1750	0.6718	2.2702	0.0039	1321.6655	0.0000	-123.8333	Cottier et al., 2006		3.9606
C. hyperboreus CV	35.8122	0.0005	4.8000	0.2828	1.7647	0.0017	20942.8109	0.0000	-126.3315	Cottier et al., 2006		27.6056
C. hyperboreus CIV	23.5337	0.0004	3.4000	0.1414	1.2500	0.0004	61930.8189	0.0000	-125.3972	Cottier et al., 2006		18.1408
C. hyperboreus CIII	4.4611	0.0001	2.5000	0.0000	0.9191	0.0001	32802.5535	0.0000	-149.3969	Cottier et al., 2006		3.4388
Metridia longa AM	31.3952	0.0005	2.6250	0.0000	1.0295	0.0004	72590.0497	0.0000	-138.6747	Cottier et al., 2006		24.2008
M. longa AF	101.7456	0.0015	1.9750	0.0000	0.7746	0.0009	110653.1910	0.0001	-139.9639	Cottier et al., 2006		78.4298
M. longa CV	495.9814	0.0075	1.8500	0.0000	0.7256	0.0004	1167015.1442	0.0006	-134.5776	Cottier et al., 2006		382.3235
M. longa CIV	277.6477	0.0042	1.3200	0.0000	0.5177	0.0003	920888.0319	0.0005	-144.9188	Cottier et al., 2006		214.0227
M. longa CIII	376.6014	0.0057	0.9000	0.0000	0.3530	0.0001	2633576.3152	0.0015	-152.6429	Cottier et al., 2006		290.3004
Paraeuchaeta spp. CV	12.5059	0.0002	4.2750	0.0200	1.6767	0.0026	4764.1650	0.0000	-132.2257	Cottier et al., 2006		9.6401
Paraeuchaeta spp. CIV	15.2556	0.0002	2.8400	0.0200	1.1139	0.0009	17518.3505	0.0000	-140.0729	Cottier et al., 2006		11.7596
Paraeuchaeta spp. CIII	0.4107	0.0000	1.8850	0.0100	0.7393	0.0002	2111.7151	0.0000	-164.9679	Cottier et al., 2006		0.3166
Paraeuchaeta spp. CII	3.9249	0.0001	1.4150	0.0100	0.5550	0.0000	392489.0346	0.0002	-161.7914	Cottier et al., 2006		3.0255
Paraeuchaeta spp. CI	9.8400	0.0001	1.0700	0.0200	0.4197	0.0006	16965.5172	0.0000	-164.3663	Cottier et al., 2006		7.5851
Bradyidius similis CV	1.6770	0.0000	1.8100	0.1350	0.7099	0.0020	846.9508	0.0000	-159.7880	Cottier et al., 2006		1.2927
Metridia lucens CVIF	168.9778	0.0025	1.5170	0.0600	0.5950	0.0000	4332765.0194	0.0024	-143.8314	Cottier et al., 2006		130.2553
Metridia lucens CVIM	79.7010	0.0012	1.2400	0.0000	0.4863	0.0000	3622772.8786	0.0020	-151.8055	Cottier et al., 2006		61.4369
Pleuromamma robusta CVIF	6.6400	0.0001	2.3500	0.0800	0.9217	0.0002	27235.4389	0.0000	-147.8881	Cottier et al., 2006		5.1184
Themisto abyssorum	5.7318	0.0001	7.8380	1.9721	2.4594	0.0350	163.9608	0.0000	-123.8267	Cottier et al., 2006		4.4183
Thysanoessa longicaudata	1.8618	0.0000	9.2165	3.1714	1.0473	0.0177	105.1114	0.0000	-99.6582	Cottier et al., 2006		1.4352
Euphausiacea furcilla	247.6399	0.0037	5.4150	1.0377	0.6153	0.0463	5352.2194	0.0000	-111.7233	Cottier et al., 2006		190.8913
Eupagurus zoea	3.4744	0.0001	1.4500	0.0500	1.1076	0.0000	185797.0778	0.0001	-149.5165	Cottier et al., 2006		2.6782
Hyas zoea	0.6680	0.0000	3.6050	0.3748	2.7538	0.0001	5536.8459	0.0000	-138.4092	Cottier et al., 2006		0.5149
Decapoda indet. Larvae	24.1338	0.0004	1.9871	0.5392	0.1926	0.0001	373819.0521	0.0002	-173.0090	Cottier et al., 2006		18.6033
Aglantha digitale	5.2180	0.0001	11.8500	3.2130	4.7400	0.0361	144.4016	0.0000	-125.8192	Stanton et al., 1994		4.0222
Sarsia sp.	0.9399	0.0000	11.0000	0.0000	4.4000	0.0336	28.0158	0.0000	-133.6356	Stanton et al., 1994		0.7245
Hydrozoa medusae indet.	864.9405	0.0130	4.0000	0.0000	1.6000	0.0122	70914.2039	0.0000	-120.4531	Stanton et al., 1994		666.7329
Siphonophorae indet.	207.8991	0.0031	1.5000	0.0000	0.6000	0.0046	45492.1488	0.0000	-148.3964	Stanton et al., 1994		160.2575
Clione limacina	0.3071	0.0000	11.7819	2.6184	11.7819	0.0858	3.5797	0.0000	-142.4048	Stanton et al., 1994		0.2367
Limacina retroversa	130.3080	0.0020	2.0000	0.3536	2.0000	0.0013	100236.9390	0.0001	-107.0255	Stanton et al., 1994		100.4470
Tomopteris sp.	2.3936	0.0000	11.5000	0.0000	0.6705	0.0143	167.9729	0.0000	-153.3295	Stanton et al., 1994		1.8451
Eukrohnia hamata	129.5984	0.0020	19.8384	5.0925	1.0609	0.0194	6666.3198	0.0000	-125.2532	Cottier et al., 2006		99.9000
Sagitta elegans	0.1115	0.0000	25.1140	5.2850	1.3430	0.0274	4.0636	0.0000	-150.7773	Cottier et al., 2006		0.0860
Oikopleura spp.	9437.6262	0.1420	3.0000	0.0000	1.5000	0.0000	403317356.8622	0.2228	-127.8094	Stanton et al., 1994		7274.9228
Pisces larvae	23.1807	0.0003	13.5696	2.9221	-	0.0224	1035.2549	0.0000	-59.0583	Chu et al., 2003		17.8687
Turbellaria	28.2705	0.0004	3.1091	2.7848	0.1813	0.0006	50483.0809	0.0000	-173.6137	Stanton et al., 1994		21.7921